NG stand mechanical interface analysis for vehicle integrated RBS 70 NG

Analys av NG stativets infästning för ett fordon integrerat RBS 70 NG

Adnan Dugalic

Faculty of Health, Science and Technology

Degree Project for Master of Science in Engineering, Mechanical Engineering

30 hp

Supervisor: Mahmoud Mousavi

Examiner: Jens Bergström

Date: 2018-06-24

Serial number: N/A

ABSTRACT

RBS 70 was introduced 1978 in Sweden and developed to be counter threats on the battlefield. This weapon is efficient against both conventional and small targets. Main components of the system are stand, sight and missile in container. RBS 70 NG with three legs is named as MANPADS configuration and has requirements for the natural frequency in launching direction to 4-6 Hz when placing it to a concrete ground.
This Master Thesis has focus on vehicle integrate system, which requires legs to be removed from the MANPADS configuration and put it on a platform placed on a vehicle. For the vehicle integrated system 3.5 Hz will be acceptable as the lowest natural frequency.
Four different concepts were purposed and evaluated for the mechanical interface between RBS 70 NG system and weapon platform:

- Existing platform with fix interface between RBS 70 NG system and platform where the thickness of the roof plate is 5 mm (named as reference model).
- Modified platform with thick plate (thickness of 30 mm) and fix interface between RBS 70 NG system and platform.
- Existing platform with damped interface between RBS 70 NG system and platform where the thickness of the roof plate is 5 mm.
- Modified platform with thick plate (thickness of 30 mm) and damped interface between RBS 70 NG system and platform.

The final concept should meet the main requirements of SMU (Stabilized Mirror Unit) and simultaneously keep natural frequency for RBS 70 NG system within requirements.
A theoretical evaluation of the longitudinal stiffness for the dampers has been calculated in the report and inputted as the value of the dampers in ANSYS R18.1. Modal analysis and harmonic response analysis was performed for all proposed concepts.
Magnification ratio calculation for a system without dampers will illustrate that the upcoming amplitude for the 5 mm plate will amplified more than 30 mm plate at coherent frequencies.
By studying the results it illustrates that a plate with thickness of 30 mm helps to minimize the disturbance in elevation direction but not in azimuth direction. To minimize the disturbance in all directions concepts with dampers will be a satisfied solution.

SAMMANFATTNING

RBS 70 introducerades 1978 i Sverige och utvecklades som ett luftvärnsystem på slagfältet. Detta vapen är effektivt mot både konventionella och små mål. Huvudkomponenterna i systemet är stativet, siktet och missilen i behållaren. RBS 70 NG är sammankopplad till tre ben som benämns som MANPADS-konfigurationen och har krav på den naturliga frekvensen i skjutriktningen till 4-6 Hz när den placeras på betongmark.
Detta examensarbete har ett fokus på fordonsintegreringssystemet, vilket kräver att benen tas bort från MANPADS-konfigurationen och RBS 70 NG systemet skall sättas på plattformen som i sin tur placeras på ett fordon. För fordon integrerade systemet är 3.5 Hz ett acceptabelt värde på den lägsta naturliga frekvensen.
Fyra olika lösningar föreslogs och uträknades för det mekaniska gränssnittet mellan RBS 70 NG-systemet och vapenplattformen:

- Befintlig plattform med fixeringsgränssnitt mellan RBS 70 NG-systemet och plattformen där takplattans tjocklek är 5 mm (benämnd som referensmodell).
- Modifierad plattform bestående av en platta med tjockleken 30 mm och ett fixeringsgränssnitt mellan RBS 70 NG-systemet och plattformen.
- Befintlig plattform med dämpat gränssnitt mellan RBS 70 NG-systemet och plattformen där takplattans tjocklek är 5 mm.
- Modifierad plattform bestående av en platta med tjockleken 30 mm samt ett dämpat gränssnitt mellan RBS 70 NG-systemet och plattformen.

Det slutliga konceptet ska uppfylla huvudkraven på SMU (Stabilized Mirror Unit) och samtidigt behålla den naturliga frekvensen för RBS 70 NG-systemet inom kravramen.
En teoretisk uträkning av längdsstyvheten för dämparna har beräknats i rapporten och matades in i ANSYS R18.1. Modal analys och harmonisk responsanalys genomfördes på alla förslagna koncept.
Beräkningen av förstärkningsfaktorn för ett system utan dämpare kommer att illustrera att amplituden för en 5 mm platta förstärks mer jämfört med en 30 mm platta vid koherenta frekvenser.
Genom att studera resultaten illustreras det att en platta med tjocklek på 30 mm bidrar till att minimera störningen i höjdled men inte i azimut riktning. För att minimera störningarna i alla riktningar kommer konceptet med dämpare att vara en satisfierad lösning.

Contents

ACKNOWLEDGEMENT

I want to thank my supervisor Alem Buljubasic at SAAB Dynamics. He has helped me to understand the basic features of the RBS 70 NG system and has also helped me to solve the upcoming problems during the project. I want to thank the manager of the mechanical department Jesper Lönnroos at SAAB Dynamics for helping me with administrative cases and for giving me the opportunity to execute my Master Thesis at SAAB Dynamics. I want also to thank my supervisor Mahmoud Mousavi at Karlstad University for pushing me forward through the project and helping me understand basic knowledge in mechanical vibration.

LIST OF ABBREVIATIONS

RBS 70 NG	Robot system 70 New Generation
NG stand	New Generation stand
NG sight	New Generation sight
MANPADS	Man-portable air-defense system
LTU	Laser Transmitter Unit
NGOU	New Generation Optics Unit
SMU	Stabilized Mirror Unit
TI	Thermal Imaging
IFF	Identification, Friend or Foe
CATIA V5 R22	Computer Aided Three-dimensional Interactive Application Version5 Release22
ANSYS R18.1	Analysis System Release18.1
CG	Center of gravity
MR	Magnification ratio
acc1	Accelerometer placed at the sight during experimental test
acc2	Accelerometer placed at the stand during experimental test
acc3	Accelerometer placed at the circular plate during experimental test
acc4	Accelerometer placed at the beams under the roof of the platform during experimental test
MATLAB R2015a	Matrix Laboratory Release 2015, first edition
point1	A point marked at the circular plate for measuring the upcoming amplitude response
point2	A point marked at the stand for measuring the upcoming amplitude response
point3	A point marked at the sight for measuring the upcoming amplitude response
PSD	Power Spectral Density

LIST OF VARIABLES

Variable	Description	Unit
k	Stiffness of the RBS 70 NG system	$[\frac{\mathrm{N}}{\mathrm{m}}]$
u_1	Displacement of the 5 mm thick platform	[m]
u_2	Displacement of the 30 mm thick platform	[m]
b_1	Amplitude for the movement of the 5 mm thick platform	[m]
b_2	Amplitude for the movement of the 30 mm thick platform	[m]
ω_1	Excitation frequency for thin plate (thickness of 5mm)	[Hz]
ω_2	Excitation frequency for thin plate (thickness of 30mm)	[Hz]
C	Damping coefficient	$[\frac{\mathrm{N*s}}{\mathrm{m}}]$
x	Displacement of RBS 70 system in x direction	[m]
t	Time	[s]
X	Maximum amplitude	[m]
$\frac{dx}{dt}$	Velocity in x direction	$[\frac{\mathrm{m}}{\mathrm{s}}]$
$\frac{d^2x}{dt^2}$	Acceleration in x direction	$[\frac{\mathrm{m}}{\mathrm{s^2}}]$
m	Mass of the RBS 70 NG system	[kg]
ω_n	Angular natural frequency	$[\frac{\mathrm{rad}}{\mathrm{s}}]$
f	Natural frequency	[Hz]
z	Relative motion	[m]
ζ	Damping ratio	-
e	Distance between dampers	[m]
a	Distance from the plate to the center of gravity	[m]
m_1	Mass of the robot tube	[kg]
m_2	Mass of the sight	[kg]
m_3	Mass of the stand, human body and IFF	[kg]
I	Moment of inertia	[kg*m^2]
$w(x,y,t)$	Transverse deflection	[m]
E	Young's modulus	[Pa]
υ	Poisson's ratio	-
ρ	Density	$[\frac{\mathrm{kg}}{\mathrm{m^3}}]$
D	Bending rigidity	[Pa*m^3]
v_0	Initial velocity	$[\frac{\mathrm{m}}{\mathrm{s}}]$

w_0	Initial deflection	[m]
$W(x,y)$	Shape function	[m]
E	Energy of a spring	[J]
i	Plate length	[m]
j	Plate width	[m]
∇^2	Laplace operator	-
A	Arbitrary constant which depends on the initial condition of motion	-
B	Arbitrary constant which depends on the initial condition of motion	-
c_{mn}	Vibration amplitude for each mode shape	[m]
Δ	Determinant	-
$\frac{\partial w}{\partial t}$	Velocity in transverse direction	$[\frac{\mathrm{m}}{\mathrm{s}}]$
m	A value to illustrate the different mode shapes	-
n	A value to illustrate the different mode shapes	-
β	Stiffness coefficient	$[\frac{1}{\mathrm{Hz}}]$
ω_3	Lower limit value of the frequency range	[Hz]
ω_4	Upper limit value of the frequency range	[Hz]
Q	Work	[J]
s	Deformation of the dampers	[m]
F	Force	[N]
$k_{minimal}$	The lower theoretical limit for damping stiffness	$[\frac{\mathrm{N}}{\mathrm{m}}]$
$k_{maximal}$	The upper theoretical limit for damping stiffness	$[\frac{\mathrm{N}}{\mathrm{m}}]$

1. INTRODUCTION

Saab Dynamics is the manufacturer of the RBS 70 NG system, which is the new generation of the well-known RBS 70 system. In order to stay ahead of the constantly developing threats on the battlefield, RBS 70 has continuously been upgraded and improved since its introduction in Sweden in 1978.
This variant compared to RBS 70 system is equipped with a new sight, which makes it possible to use the function of automatic target tracking instead of manual tracking [1]. Another feature in the new system is an integrated thermal imager, which give some advantageous for the user to see through smoke and the system can be used at nights [2]. RBS 70 NG system is efficient against both conventional and small targets. The missile can be used against aerial "armoured" targets such as attack helicopters, close air support aircrafts and also ground targets (see figure 1).

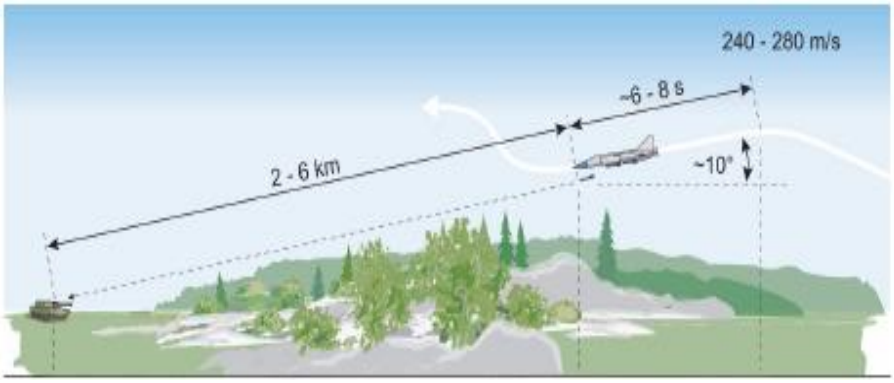

Figure 1. Combat aircraft attacking at low altitude [3].

The main components of the system are shown in figure 2.

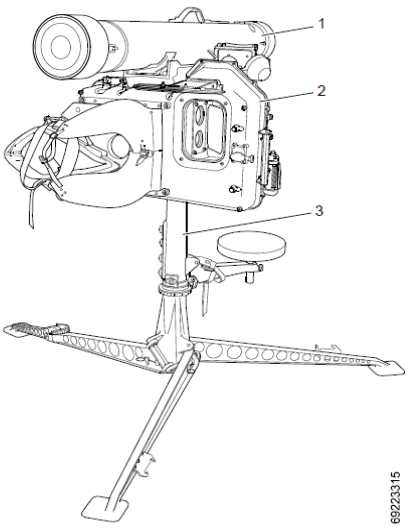

1. Missile in container
2. NG Sight
3. NG Stand

Figure 2. MANPADS configuration [4].

The three main components are sight, stand and missile in container which build up a firing unit (see figure 2). The stand has three legs and rough levelling is carried out by adjusting one of the legs. The sight and the missile in the container are attached to the stand.

The missile is launched from the container and only removed from the container at the moment of firing. The container main purpose is for storage and transport. A launch motor, which burns out in the launch tube, ejects the missile and separates from it a short distance from the tube, after the sustainer motor takes over. The end covers on both side of the container are tightly closed by sealing rings against the inside of the launching tube and have the function to protect the missile against water and humidity. Each end cap is constrained by two clamps and on loading the caps are removed. A handle on the container is used for short transport and an illustration is shown in figure 3.

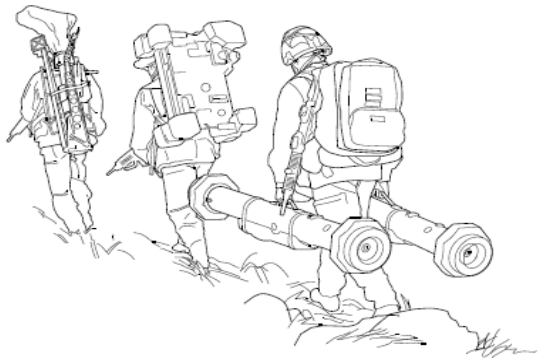

Figure 3. RBS 70 NG being carried [3].

Another important part of the system is the sight. The sight casing consists of two parts, front casing and rear casing, which are screwed and sealed together. The casing of the sight has the function to withstand environmental stresses and provides a surface for mounting other components. The attachment for the sight to the stand is by brackets and secured by a catch. The transmitter in the sight consists of a Laser Transmitter Unit (LTU), which has the function to generate a beam. The beam is then transmitted to the NG Optics Unit (NGOU) where the zoom unit, which is a part of the NGOU, has the function to find the missile upon launching and subsequently zoom onto the target. This beam are then reflected by a Stabilized Mirror Unit (SMU) and transmitted through the front sight window. The mirror can rotate around azimuth axis and elevation axis (see figure 4). Two gyros are mounted to control the azimuth angle and elevation angle.

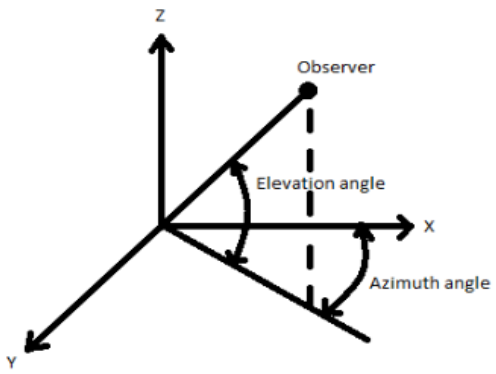

Figure 4. The azimuth angle and elevation angle.

If the mirror approaches a maximum deflection, the operator will receive a message in the display to rotate the sight in same direction as the mirror has been rotated. The mirror's secondary function is to reflect the incoming IR radiation to the Thermal Imaging (TI), which makes it able to see objects through eyepiece in the IR spectrum. The incoming IR radiation and the guidance beam are synchronized when reaching the mirror. The system as mentioned before has automatic target tracking and also manually target tracking by using a thumb joystick to aim at objects.

The function for the stand is to support the sight and missile in the firing operation and during transportation the stand is folded [4].

RBS 70 NG system has been integrated with IFF system with adaptions for RBS 70. Identification Friend or Foe (IFF) is a system to identify aircraft or vehicles as friendly.

The MANPADS system is used on a hard ground and in launching direction the natural frequency should lay between 4-6 Hz. A low natural frequency for example a value of 2 Hz will result in large displacement of sight which is unacceptable, but should not exceed 6 Hz because the stand becomes more rigid and leads to nose up rotation of the robot [5]. The stiffness of the platform cannot be considered as unlimited stiff and investigation performed by SAAB Dynamics will change the lower requirements for natural frequency to >3.5 Hz [6].

For the vehicle integrated system it is required to remove the legs from the MANPAND system and put it on a platform placed on a vehicle. A schematic picture of the vehicle integrated system is shown in figure 5.

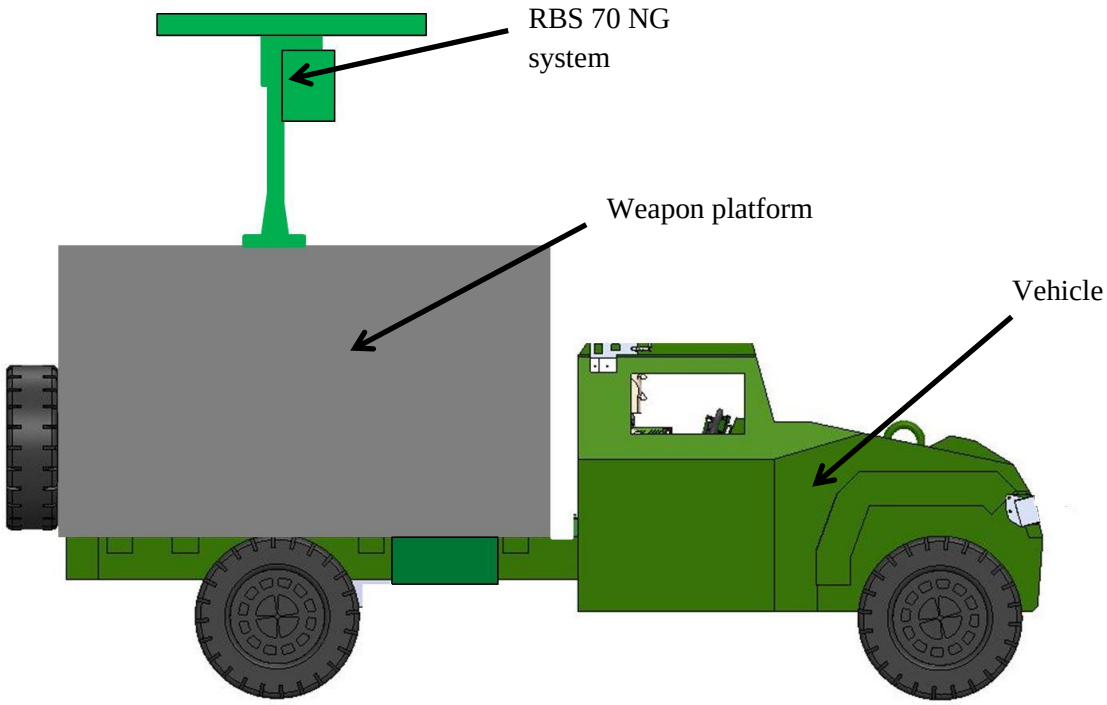

Figure 5. Vehicle integrated robot 70 NG.

The upcoming sound waves during launching will generate vibration on the roof of the weapon platform. This may disturb the system and the two gyros of the SMU cannot meet the requirement.

1.1 PROBLEM FORMULATION

This Master Thesis will investigate and propose solutions for mechanical interface between RBS 70 NG system and weapon platform. The solution should meet main requirements for SMU and simultaneously keep the lowest natural frequency for RBS 70 NG system between 3.5 (4)-6 Hz in launching direction. It will be simulated in the software ANSYS R18.1 and compared with the theory to analyze the accuracy. Firing exercise was performed during development of the original weapon platform and the measurement will be reused in this Master Thesis. This report will also include suggestion on design changes on the original weapon platform by using CATIA V5 R22 software and the drawing will be added.

2. THEORY

This chapter will carry out theoretical evaluations and compare it with simulations in ANSYS R18.1. The following reference model is studied:

Existing platform with fix interface between RBS 70 NG system and platform (the thickness of the roof plate is 5 mm).

Further, three design solutions (concepts) are suggested:

a) Modified platform with thick plate (thickness of 30 mm) and fix interface between RBS 70 NG system and platform.
b) Existing platform with damped interface between RBS 70 NG system and platform (the thickness of the roof plate is 5 mm).
c) Modified platform with thick plate (thickness of 30 mm) and damped interface between RBS 70 NG system and platform.

2.1 THEORETICAL EVALUATIONS

The reference model is illustrated in figure 6. The mass includes the stand, sight and robot tube. Note that the mass of the missile is not included in the model due to consideration of the problem after launching. Stiffness of the RBS 70 NG system is represented as spring and denoted by k. The roof is exciting by generation of thrust when launching the robot and the movement can be expressed as $u_1 = b_1 * sin(\omega_1 t)$. To keep things simple the stative, sight and robot tube are named as system.

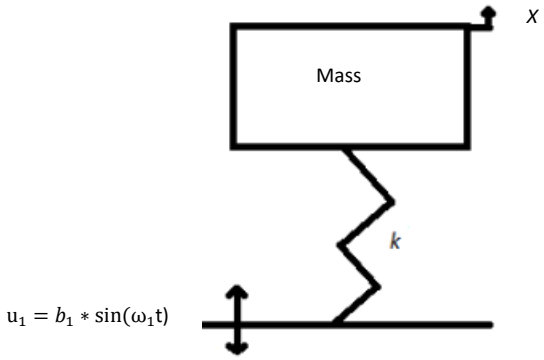

Figure 6. A 5 mm thick roof (reference model).

Other concepts mentioned before have been developed to improve the reference system.
The concept a) is shown in figure 7 and illustrates the reference system modified by using a plate with thickness of 30 mm and is mounted on the roof of the platform, which is exciting by generation of thrust when launching the robot. The excitation movement can be expressed as $u_2 = b_2 * sin(\omega_2 t)$. Note that parameters mass and spring are considered in same way as in the reference system. The excitation frequency ω_2 is higher than ω_1 because of a more stiffener structure.

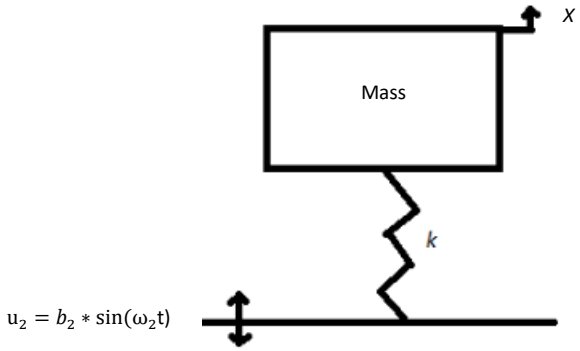

Figure 7. Modified roof with thickness of 30 mm (concept a).

The concept b) is described in figure 8. This concept is represented as the reference system but with addition of a damper, denominate as *C* in figure 8. The exciting movement is described as $u_1 = b_1 * sin(\omega_1 t)$. Note that parameters mass and spring are considered in same way as in the reference system.

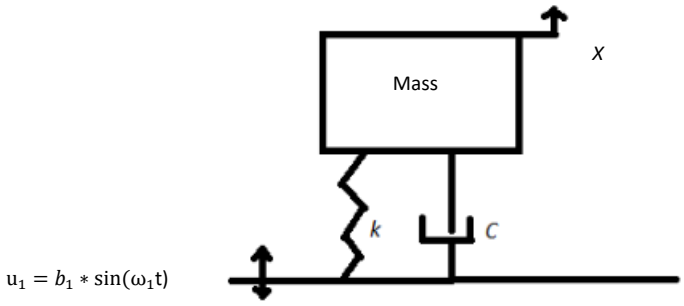

Figure 8. A 5 mm thick roof with damped interface (concept b).

The concept c) is described in figure 9. This concept represents the system by introducing a damper at the interface and also a 30 mm thick plate, which is mounted on the roof of the platform. The exciting movement is described as $u_2 = b_2 * sin(\omega_2 t)$. Note also that parameters mass and spring are considered in same way as in the reference system.

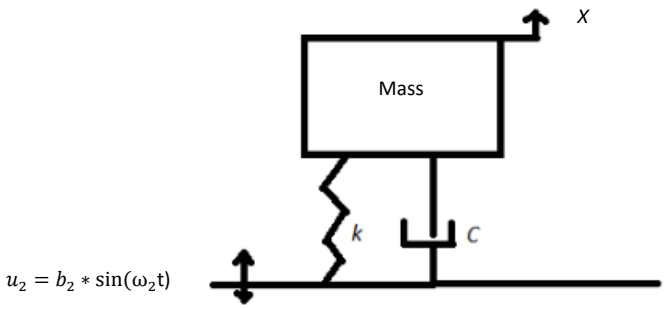

Figure 9. Modified roof with thickness of 30 mm and damped interface (concept c).

To analyze how the displacement of the system reacts on incoming vibration from the thrust, it is useful to derive and study the transmissibility. The equation of motion without damper can be described as

$$m\frac{d^2x}{dt^2} + kx = ku = kbsin(\omega t) \quad (1)$$

For this solution the motion of mass is assumed to be harmonic and can be expressed as steady state response.

$$x = Xsin(\omega t) \quad (2)$$

Where the X is the maximum amplitude. The equation (2) is differentiated twice and the solution is shown below.

$$\frac{dx}{dt} = \omega X cos(\omega t) \qquad (3)$$

$$\frac{d^2x}{dt^2} = -\omega^2 X sin(\omega t) \quad (4)$$

By substituting (4) and (2) in (1) it leads to

$$X = \frac{kb}{m(\frac{k}{m} - \omega^2)} \quad (5)$$

Natural frequency can be described by

$$\omega_n = \sqrt{\frac{k}{m}} \quad (6)$$

By substituting (6) in (5), the transmission ratio will end up with

$$\frac{X}{b} = \frac{1}{1 - \frac{\omega^2}{\omega_n^2}} \quad (7)$$

Figure 10 shows the equation (7) in a graphically way.

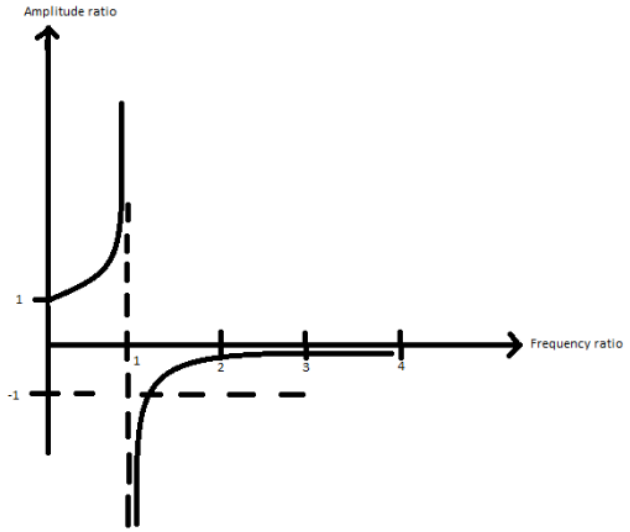

Figure 10. Forced vibration caused by harmonic ground motion without damper.

The relative motion can be described as the difference between exiting movement and the movement of the system, $z = x - u$. The magnification ratio can be expressed as

$$\frac{Z}{b} = \frac{(\frac{\omega^2}{\omega_n^2})}{(1-\frac{\omega^2}{\omega_n^2})} \quad (8)$$

Figure 11 shows the equation (8) in a graphically way.

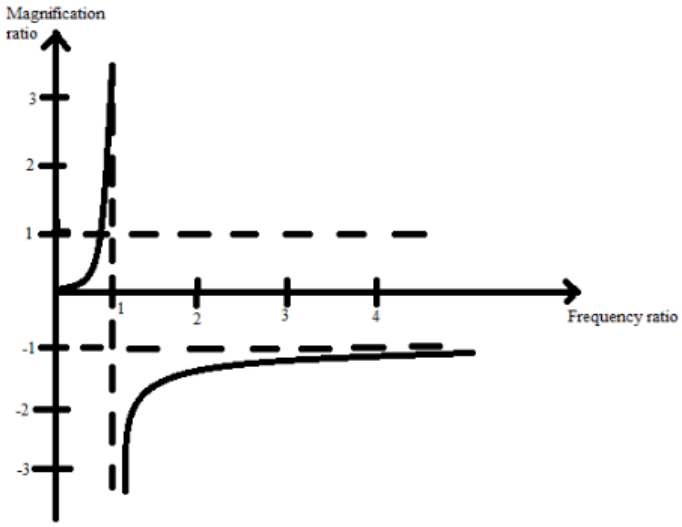

Figure 11. A plot of magnification ratio ($\frac{z}{b}$) against frequency ratio ($\frac{\omega}{\omega_n}$).

The equation of motion for forced vibration caused by harmonic motion with damper is

$$m\frac{d^2x}{dt^2} + kx + C\frac{dx}{dt} = C\frac{du}{dt} + ku \quad (9)$$

The transmission ratio for a forced damped system ends up with

$$\frac{X}{b} = \sqrt{\frac{1+(2\zeta\frac{\omega^2}{\omega_n^2})^2}{(1-\frac{\omega^2}{\omega_n^2})^2+(2\zeta\frac{\omega}{\omega_n})^2}} \quad (10)$$

Where ζ is the damping ratio [7].

Figure 12 shows the equation (10) in a graphically way.

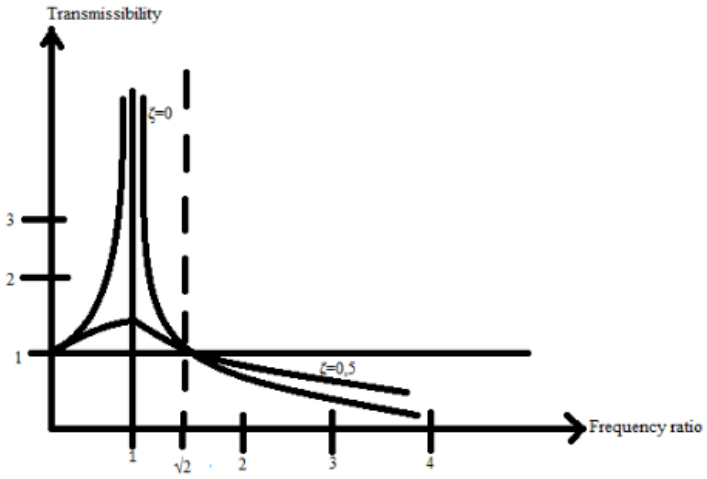

Figure 12. Forced vibration caused by harmonic ground motion with damper.

2.2 DEFINITON OF DAMPERS

To define theoretically which stiffness the dampers on the plate should have, a simplified model was constructed in launching direction and is shown in figure 13.

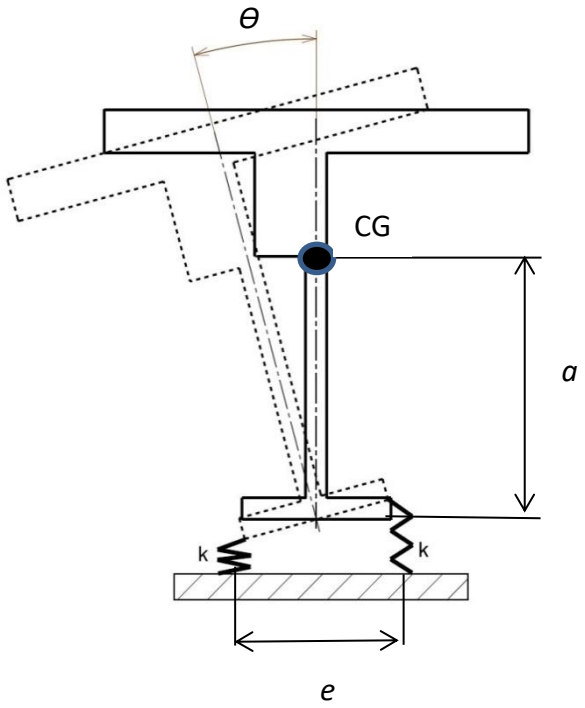

Figure 13. Damping model.

The abbreviation CG is the center of gravity and the distance between CG and the plate is denoted by alphabetic letter "*a*". The distance between the springs is denoted by alphabetic letter "*e*". The mass of system is 142 kg. To define where the CG is placed on the system a simple calculation is used by observing figure 14. For the simplified model the damping coefficient was not considered.

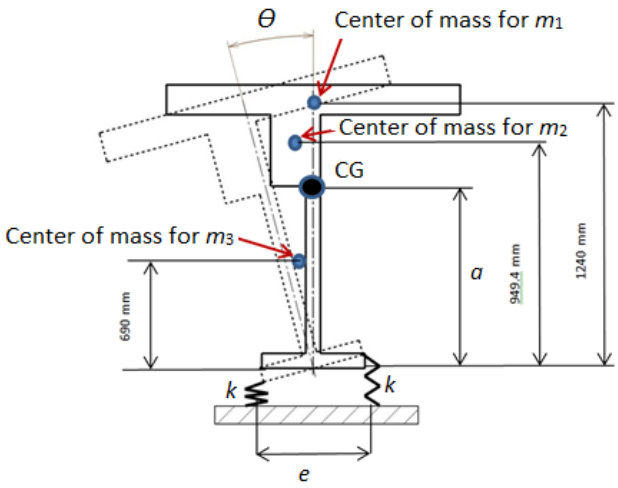

Figure 14. A model to define the placement of CG on the system.

The distance between the circular plate and the center of gravity can be expressed as

$$a = \frac{((m_1 * 1240) + (m_2 * 950) + (m_3 * 700))}{(m_1 + m_2 + m_3)} \quad (11)$$

Where the different masses are defined as
m_1- mass of robot tube = 7 kg

m_2- mass of sight = 25 kg

m_3- mass of the stand, human body and IFF = 110 kg

By inputting these values in equation (11) the center of gravity will be, a = 770 mm.

A momentum equation is expressed as the first step to find which parameters the stiffness of the dampers depends on.

$\sum M_0 = I\frac{d\theta^2}{d^2t}$, where I is moment of inertia for a point mass and are defined as $I = ma^2$ [8]. This result in

$$-ke^2\theta = I\frac{d^2\theta}{dt^2} \quad (12)$$

The equation (12) can be solved by assuming harmonic vibration

$$\theta = \theta \sin(\omega t) \quad (13)$$

The stiffness of dampers can be expressed as

$$k = \frac{\omega^2 m a^2}{e^2} \quad (14)$$

The system has demand on the first mode of natural frequency to be between 4-6 Hz according to requirements. This demand is useful for calculating $k_{minimal}$ and $k_{maximal}$ by using equation (14). Calculated $k_{minimal}$ respective $k_{maximal}$ are exposed in table 1 and table 2.

Table 1. Calculation of *kminimal*

Variable	Value	Unit
k=	470000	$[\frac{\mathrm{N}}{\mathrm{m}}]$
e=	0.35	[m]
a=	0.77	[m]
m=	142	[kg]
ω^2=	635.4	$[\frac{\mathrm{rad}}{\mathrm{s}}]$
ω=	25.2	$[\frac{\mathrm{rad}}{\mathrm{s}}]$
f=	4.0	[Hz]

Table 2. Calculation of *kmaximal*

Variable	Value	Unit
k=	1050000	$[\frac{\mathrm{N}}{\mathrm{m}}]$
e=	0.35	[m]
a=	0.77	[m]
m=	142	[kg]
ω^2=	1423	$[\frac{\mathrm{rad}}{\mathrm{s}}]$
ω=	37.7	$[\frac{\mathrm{rad}}{\mathrm{s}}]$
f=	5.99	[Hz]

The demand is fulfilled if the stiffness of the dampers varies between $470000 \leq k < 1050000$, where the unit of *k* is expressed in $\frac{\mathrm{N}}{\mathrm{m}}$.

2.3 PLATE THEORY

To illustrate a 3D model, a plate with arbitrary supports was considered. The plate can be seen as a continuous elastic system, because it is a structure [9]. Therefore the plate can be described by mathematically partial differential equations. For free vibration the forced part is set to zero and the resulting differential equation is shown in equation (15). Note that the plate is isotropic and homogenous.

$$D\nabla^2\nabla^2 w(x,y,t) + \rho h \frac{\partial^2 w}{\partial t^2}(x,y,t) = 0 \quad (15)$$

Where $w(x,y,t)$ is transverse deflection; $\nabla^2 = \frac{\partial^2}{\partial x^2} + \frac{\partial^2}{\partial y^2}$ is Laplace operator where x and y is Cartesian coordinates in x-y plane [10]; $D = \frac{Eh^3}{12(1-\upsilon^2)}$ is the bending rigidity where *E*=Young's modulus, Poisson ratio is υ and *h* is the thickness of the plate; ρ is the density of the plate [11].

The deflection need to satisfy the boundary condition at the plate edges; $t=0$: $w = w_0(x,y)$,

$\frac{\partial w}{\partial t} = v_0(x, y)$. Where v_0 and w_0 are the initial velocity and initial deflection.

The deflection can be assumed to depend on a harmonic response over time and a shape function $W(x, y)$ as expressed in equation (16).

$$w(x, y, t) = (A\cos(wt) + B\sin(wt))W(x, y) \quad (16)$$

By differentiating the equation (16) twice and then replace it in equation (15) this will end up with

$$D\nabla^2\nabla^2 W(x, y) - \omega^2\rho h W = 0 \quad (17)$$

To calculate the natural frequency the system determinant should be equal to zero.

$$\Delta(w) = 0 \quad (18)$$

For each natural frequency there is a corresponding shape function and for the case with rectangular plate which is simple supported, the shape function is expressed as

$$W(x, y) = \sum_{m=1}^{\infty}\sum_{n=1}^{\infty} c_{mn}\, sin\frac{m\pi x}{i} sin\frac{n\pi y}{j} \quad (19)$$

Where c_{mn} is the vibration amplitude for each value of *m* and *n*. The dimensions of the plate are expressed as *i* and *j*. The equation (19) can be input in (17) and that results in

$$\omega_{mn} = \pi^2\left(\frac{m^2}{i^2} + \frac{n^2}{j^2}\right)\sqrt{\frac{D}{\rho h}} \quad (20)$$

Equation (20) describes the natural frequency for a rectangular plate and depends on geometry as well as material parameters [12]. The lowest frequency can be defined by putting *m*=1 and *n*=1, so the expression results in

$$\omega_{11} = \pi^2\left(\frac{1}{i^2} + \frac{1}{j^2}\right)\sqrt{\frac{D}{\rho h}} \quad (21)$$

By using equation (21) the natural frequency for the first mode can be calculated to 52 Hz for an aluminum plate with a thickness of 5 mm and the calculation is shown in table 3.

Table 3. Theoretical calculation of natural frequency for the first mode (thickness 5 mm)

Variable	Value	Unit	Description
$m=$	1	-	A value illustrating different mode shapes
$n=$	1	-	A value illustrating different mode shapes
$i=$	0.894	[m]	Plate length
$j=$	0.577	[m]	Plate width
$\upsilon=$	0.33	-	Poisson ratio
$E=$	$7*10^{10}$	[Pa]	Young's modulus
$\rho=$	2700	$[\frac{kg}{m^3}]$	Density
$h=$	0.005	[m]	Thickness
$D=$	818	[Pa*m³]	Bending rigidity
$\omega_{mn}=$	326.6	$[\frac{rad}{s}]$	Angular natural frequency
$f=$	52	[Hz]	Natural frequency

Figure 15 shows the calculation of natural frequency for a simply bonded aluminum plate with thickness of 5 mm by using CATIA V5 R22.

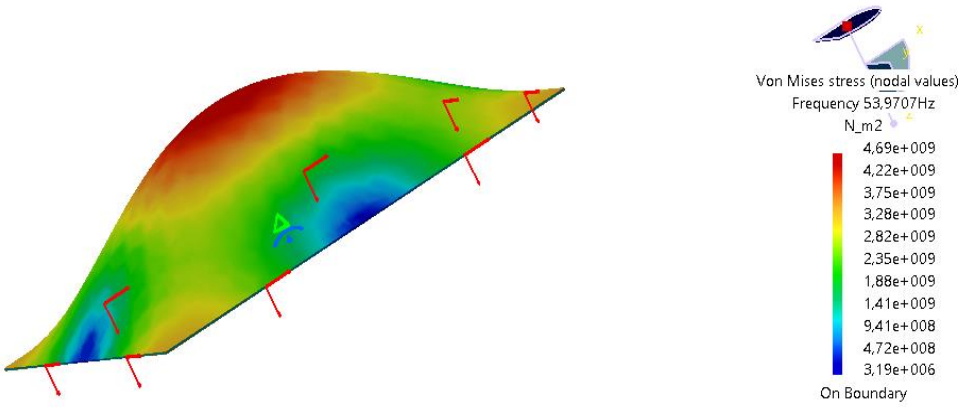

Figure 15. Calculation of natural frequency for the first mode in CATIA V5 R22 (thickness 5 mm).

The calculated values for natural frequency from the theory 52 Hz and simulation 53.9 Hz correspond to each other. Even the second mode of natural frequency corresponds to each other by analyzing table 4 and figure 16.

Table 4. Theoretical calculation of natural frequency for the second mode (thickness 5 mm)

Variable	Value	Unit	Description
$m=$	2	-	A value illustrating different mode shapes
$n=$	1	-	A value illustrating different mode shapes
$i=$	0.894	[m]	Plate length
$j=$	0.577	[m]	Plate width
$\upsilon=$	0.33	-	Poisson ratio
$E=$	$7*10^{10}$	[Pa]	Young's modulus
$\rho=$	2700	$[\frac{kg}{m^3}]$	Density
$h=$	0.005	[m]	Thickness
$D=$	818	[Pa*m^3]	Bending rigidity
$\omega_{mn}=$	614.7	$[\frac{rad}{s}]$	Angular natural frequency
$f=$	98	[Hz]	Natural frequency

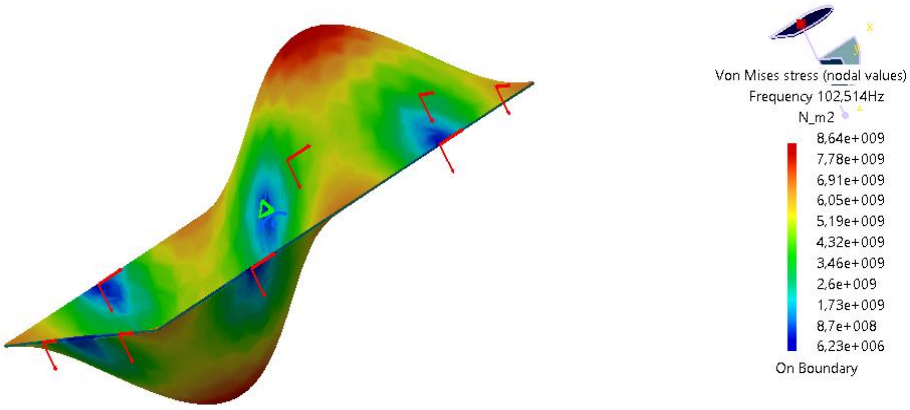

Figure 16. Calculation of natural frequency for the second mode in CATIA V5 R22 (thickness 5 mm).

If the thickness of the plate is increased to 30 mm the natural frequency is calculated by equation (21) to 312 Hz and is shown in table 5. The thickness is the only variable for the both cases with 5 mm and 30 mm plate.

Table 5. Theoretical calculation of natural frequency for the first mode (thickness 30 mm)

Variable	Value	Unit	Description
m=	1	-	A value illustrating different mode shapes
n=	1	-	A value illustrating different mode shapes
i=	0.894	[m]	Plate length
j=	0.577	[m]	Plate width
υ=	0.33	-	Poisson ratio
E=	$7*10^{10}$	[Pa]	Young's modulus
ρ=	2700	$[\frac{kg}{m^3}]$	Density
h=	0.03	[m]	Thickness
D=	176747	[Pa*m³]	Bending rigidity
ω_{mn}=	1960	$[\frac{rad}{s}]$	Angular natural frequency
f=	312	[Hz]	Natural frequency

Figure 17 shows the calculation of natural frequency for a simply bonded aluminum plate with thickness of 30 mm by using CATIA V5 R22.

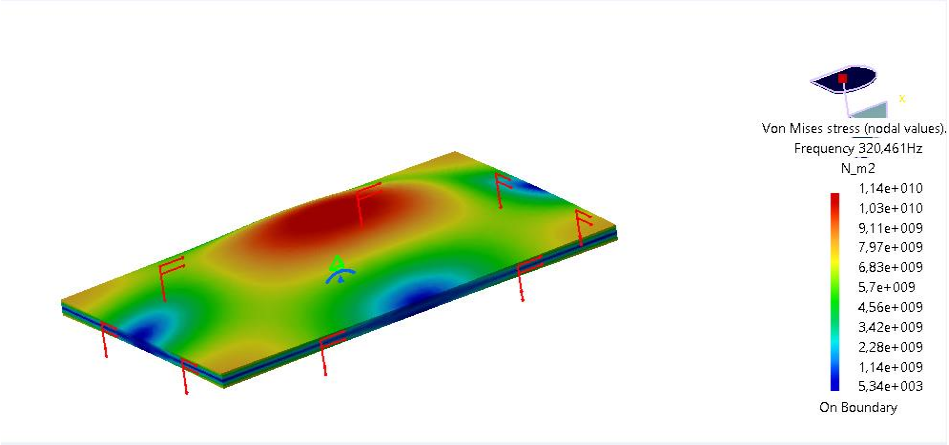

Figure 17. Calculation of natural frequency for the first mode in CATIA V5 R22 (thickness 30 mm).

The calculated values for natural frequency from the theory 312 Hz and simulation 320 Hz correspond to each other. Even the second mode of natural frequency corresponds to each other by analyzing table 6 and figure 18.

Table 6. Theoretical calculation of natural frequency for the second mode (thickness 30 mm)

Variable	Value	Unit	Description
m=	2	-	A value illustrating different mode shapes
n=	1	-	A value illustrating different mode shapes
i=	0.894	[m]	Plate length
j=	0.577	[m]	Plate width
υ=	0.33	-	Poisson ratio
E=	$7*10^{10}$	[Pa]	Young's modulus
ρ=	2700	$[\frac{kg}{m^3}]$	Density
h=	0.03	[m]	Thickness
D=	176747	[Pa*m^3]	Bending rigidity
ω_{mn}=	3688	$[\frac{rad}{s}]$	Angular natural frequency
f=	587	[Hz]	Natural frequency

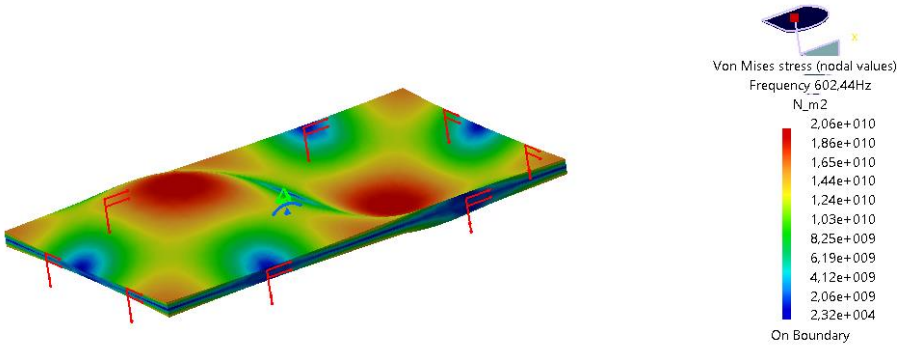

Figure 18. Calculation of natural frequency for the second mode in CATIA V5 R22 (thickness 30 mm).

By increasing thickness, the relation $\frac{\omega}{\omega_n}$ in figure 10 will increase and leads to decrease in amplitude ratio. This result in a stiffer structure and the equation (22) illustrates also that by increasing excited frequency the amplitude of the system will decrease for the same amount of energy with constant mass [13].

$$E = \frac{1}{2}kA^2 = \frac{1}{2}\omega^2 mA^2 \quad (22)$$

Table 7 illustrates calculations of magnification ratio for different exciting frequencies to study the amplitude response for a 5 mm plate.

Table 7. A range of exciting frequencies to study the amplitude response for a 5 mm plate

Excitation frequency, f_e [Hz]	Excitation frequency,$\omega_1[\frac{\text{rad}}{\text{s}}]$	$\omega_1^2/\ \omega_{11}{}^2$	$\omega_1/\ \omega_{11}$	MR=$\frac{Z}{b}$
10	63	0,036882791	0,192049	0,038295
20	126	0,147531166	0,384098	0,173063
30	188	0,331945122	0,576147	0,496883
40	251	0,590124662	0,768196	1,439766
50	314	0,922069785	0,960245	11,83199
60	377	1,32778049	1,152294	– 4,05082
70	440	1,807256778	1,344343	– 2,23876
80	502	2,360498649	1,536391	– 1,73502
90	565	2,987506102	1,72844	– 1,50314
100	628	3,688279138	1,920489	– 1,37199
110	691	4,462817758	2,112538	– 1,28878
120	754	5,311121959	2,304587	– 1,23196
130	816	6,233191744	2,496636	– 1,19109
140	879	7,229027111	2,688685	– 1,16054
150	942	8,298628062	2,880734	– 1,13701
160	1005	9,441994595	3,072783	– 1,11846
170	1068	10,65912671	3,264832	– 1,10353
180	1130	11,95002441	3,456881	– 1,09132
190	1193	13,31468769	3,64893	– 1,0812
200	1256	14,75311655	3,840979	– 1,07271

MR as mentioned before stands for magnification ratio and ω_{11} is the lowest natural frequency for a 5 mm plate. The figure 19 shows the data from table 7 and is used to build up a graph consisting of magnifications ratio on y axis as well as frequency ratio on x axis.

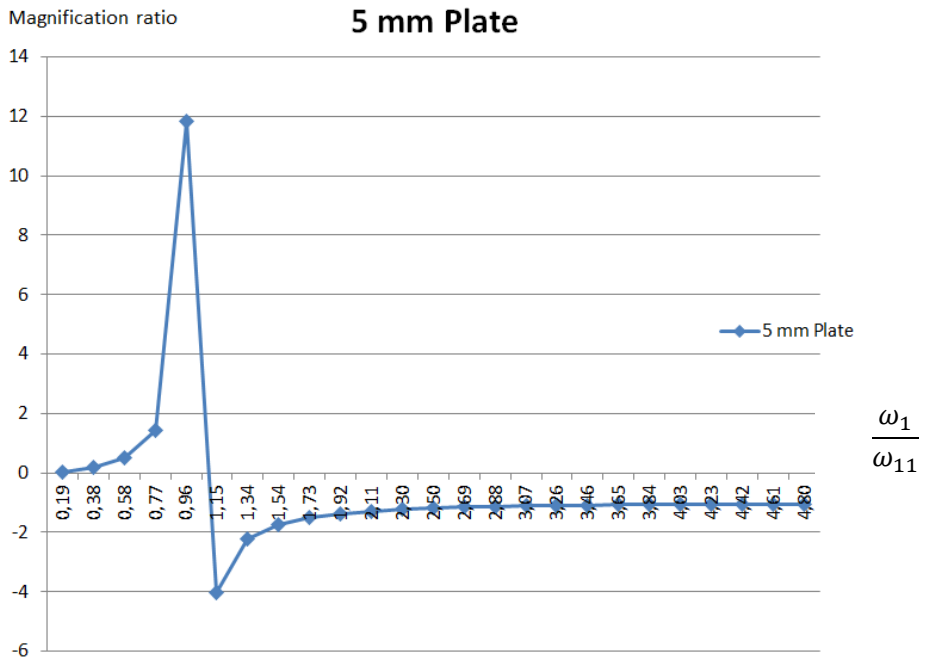

Figure 19. Magnification ratio related to frequency ratio for a plate with thickness of 5 mm.

Table 8 illustrates calculations of magnification ratio for different exciting frequencies to study the amplitude response for a 30 mm plate.

Table 8. A range of exciting frequencies to study the amplitude response for a 30 mm plate

Excitation frequency, f_e [Hz]	Excitation frequency,$\omega_2[\frac{\text{rad}}{\text{s}}]$	$\omega_2^2/\ \omega_{11}{}^2$	$\omega_2/\ \omega_{11}$	MR=$\frac{Z}{b}$
10	63	0,001027662	0,032057	0,001029
20	126	0,004110649	0,064114	0,004128
30	188	0,009248961	0,096172	0,009335
40	251	0,016442596	0,128229	0,016717
50	314	0,025691557	0,160286	0,026369
60	377	0,036995842	0,192343	0,038417
70	440	0,050355452	0,2244	0,053026
80	502	0,065770386	0,256457	0,070401
90	565	0,083240645	0,288515	0,090799
100	628	0,102766228	0,320572	0,114537
110	691	0,124347136	0,352629	0,142005
120	754	0,147983368	0,384686	0,173686
130	816	0,173674925	0,416743	0,210177
140	879	0,201421807	0,4488	0,252226
150	942	0,231224013	0,480858	0,300769
160	1005	0,263081543	0,512915	0,357002
170	1068	0,296994398	0,544972	0,422464
180	1130	0,332962578	0,577029	0,499166
190	1193	0,370986082	0,609086	0,58979
200	1256	0,411064911	0,641143	0,69798

Figure 20 shows the data from table 8 and is used to build up a graph consisting of magnification ratio on y axis as well as frequency ratio on x axis.

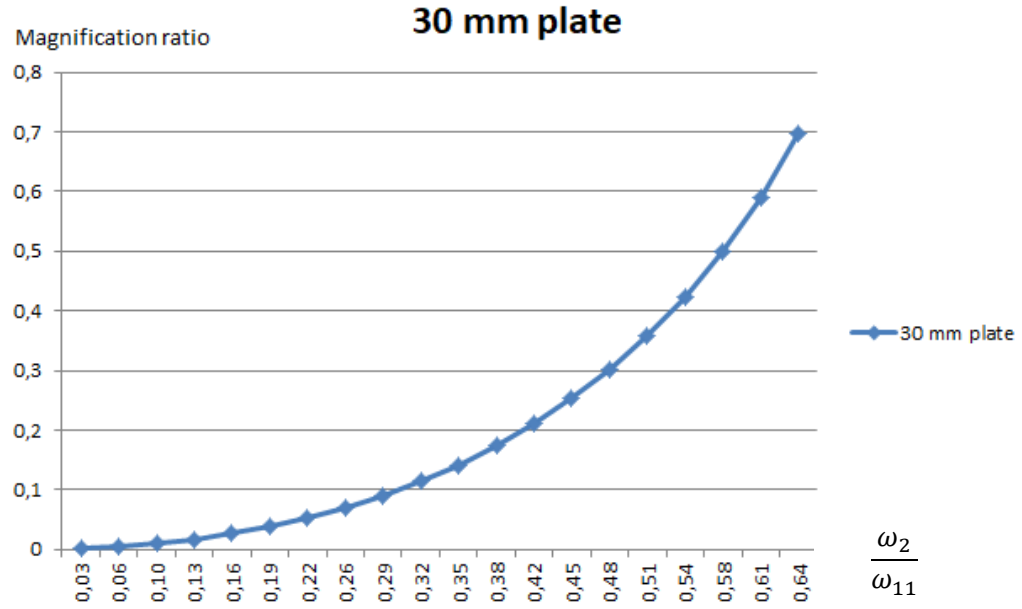

Figure 20. Magnification ratio related to frequency ratio for a plate with thickness of 30 mm.

By comparing figure 19 and 20, it expose that the upcoming amplitude of 5 mm plate is amplified more than 30 mm plate for the same frequencies band.

3. DESIGN

The design of the original platform used for experimental test is shown in figure 21.

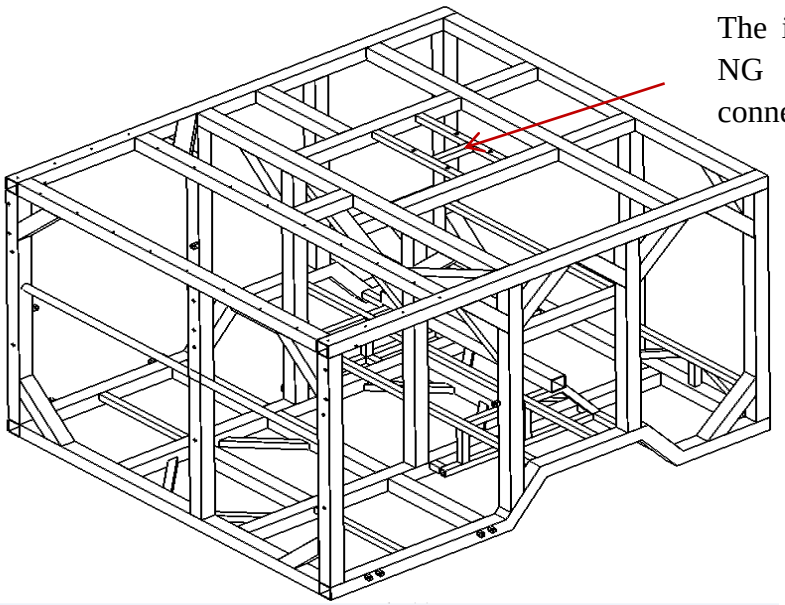

Figure 21. The design of the original platform.

The original platform was modified by replacing the three beams with four beams placed as a frame and stiffened by two transverse beams. This modification is shown in figure 22.

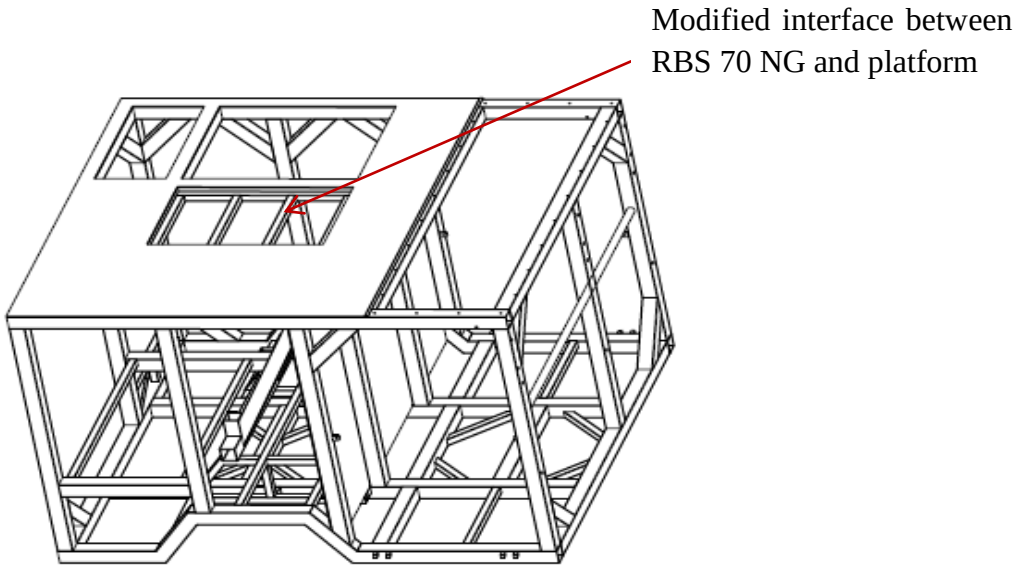

Figure 22. The design of the modified platform.

Figure 23 illustrates RBS 70 NG connected with four dampers screwed on a 30 mm thick plate. This plate is welded all around at the interface on the modified platform.

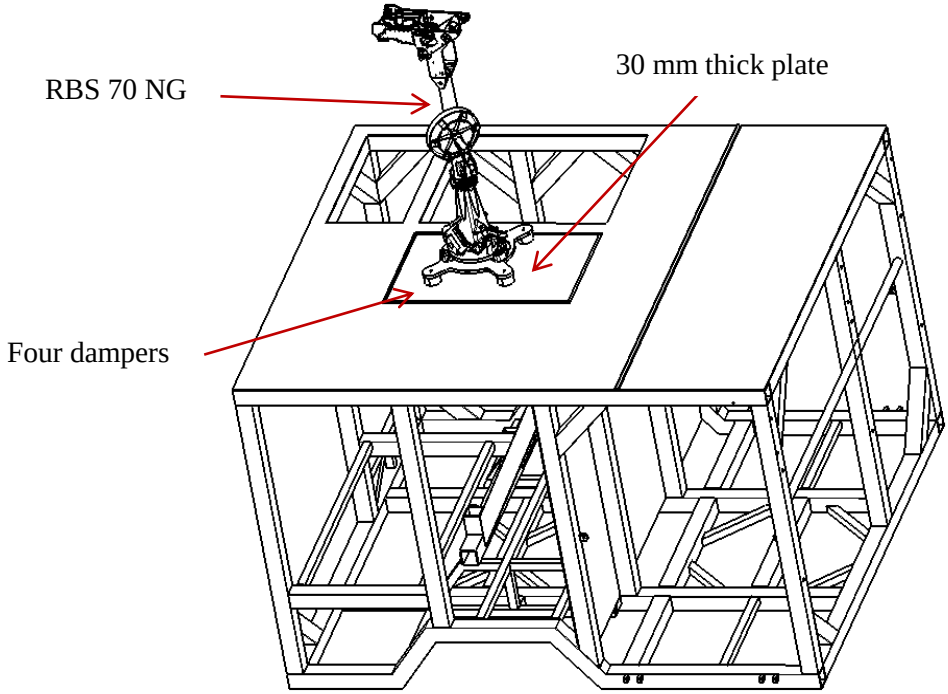

Figure 23. RBS 70 NG system placed on the modified platform.

To define the stiffness value on dampers, it is useful to use equation (14) and according to this the calculation on stiffness of the dampers shall be within in the interval $470\ \frac{N}{mm}$ and $1050\ \frac{N}{mm}$. Three different standard stiffness values are chosen $640\ \frac{N}{mm}$, $780\ \frac{N}{mm}$ and $960\ \frac{N}{mm}$ which in theory meet the requirement on natural frequency (4-6 Hz). The standard stiffness values are taken from APPENDIX A. Drawings on the 30 mm plate is illustrated in APPENDIX B.

4. METHOD

A harmonic response analysis in ANSYS R18.1 has been used as a prerequisite for a modal analysis. Input acceleration, defined as base excitation for the frequency band up to 110 Hz measured in experimental test has been used. For modal analysis it is necessary to define the coefficient β for solver type reduced damped in ANSYS R18.1 and it is calculated analytically.
The purpose of the analysis is to compare different solutions to the reference design which were tested during experimental test and is illustrated in figure 24 .This design represents the platform with thin plate (5 mm thick) placed on the platform roof and fix integrated RBS 70 NG system.

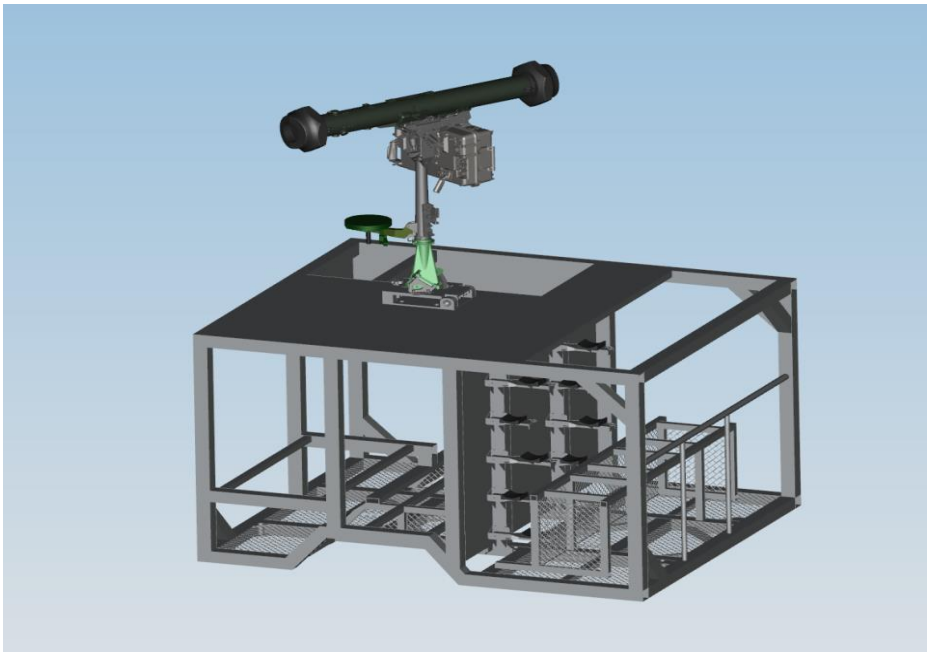

Figure 24. Existing platform with fix interface between RBS 70 NG and platform i.e. reference model.

For ANSYS R18.1 analysis the roof of the platform was only used to simplify analysis solving and mesh execution. The rest of the platform has been replaced in ANSYS R18.1 by constraints. For the same reason RBS 70 NG system is also a simplified model (see figure 25). Following solution was evaluated in ANSYS R18.1:

1. Existing platform with fix interface between RBS 70 NG and platform (the thickness of the roof plate is 5 mm) named as the reference model.
2. Modified platform with thick plate (thickness of 30 mm) and fix interface between RBS 70 NG and platform.
3. Existing platform with damped interface between RBS 70 NG and platform (the thickness of the roof plate is 5 mm).
4. Modified platform with thick plate (thickness of 30 mm) and damped interface between RBS 70 NG and platform.

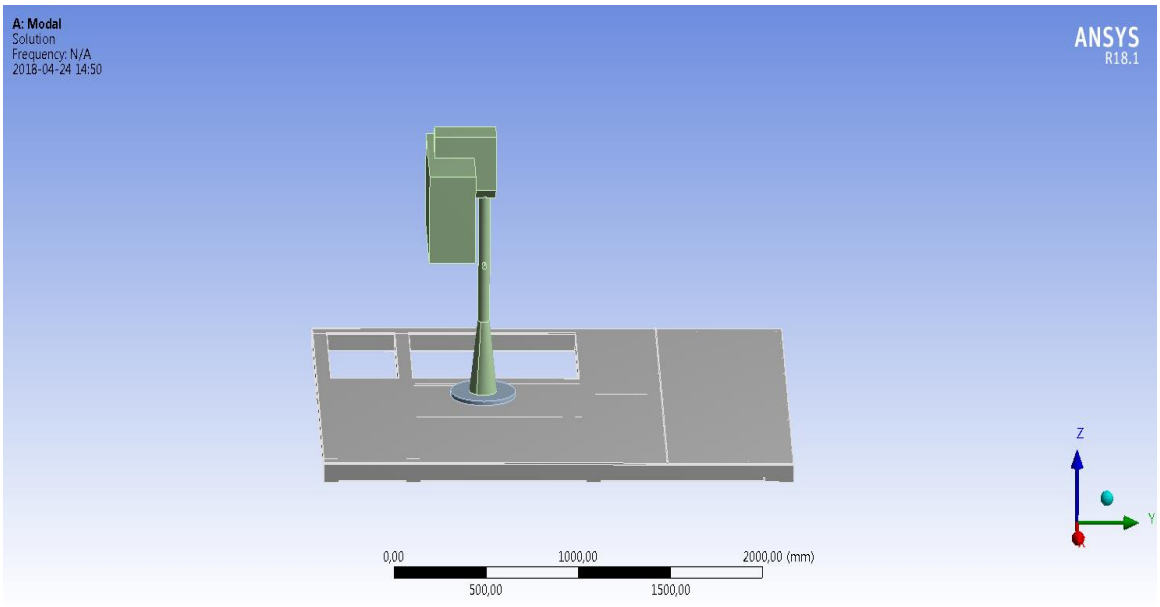

Figure 25. Simplified model for ANSYS R18.1 analysis.

The natural frequency in launching direction was experimentally tested for the MANPAD system placed on a concrete ground and the result was 4.7 Hz [14]. The simple model of RBS 70 NG was placed on three legs to compare it to the experimental test. By comparing experimental test and simulation test (see figure 26) it illustrates that the natural frequency in launching direction is approximately the same for both cases and the simple model of RBS 70 NG can be seen as valid for further simulation.

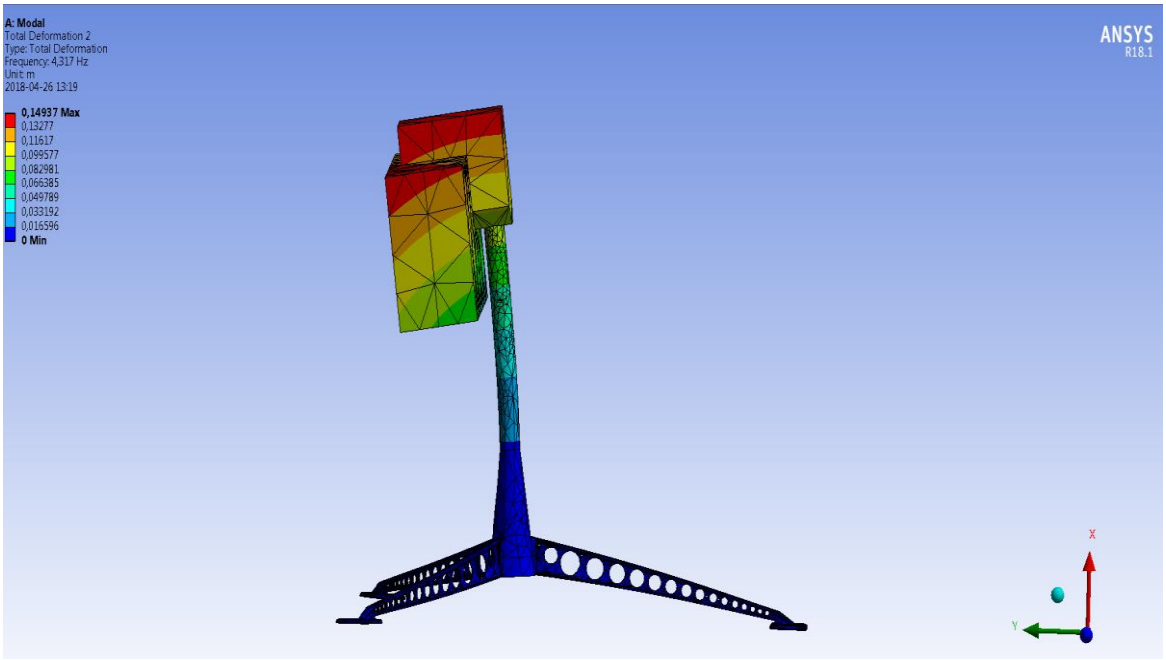

Figure 26. The natural frequency for the simple model of RBS 70 NG placed on three legs is 4.3 Hz.

4.1 MODELLING IN ANSYS

The RBS 70 NG system was modelled in CATIA V5 R22 and a step file was imported of the model into ANSYS R18.1. For this type of problem a modal analysis and harmonic response where executed.

The material for NG stand and NG sight is defined as magnesium. The other two parts, which are the roof of the platform and the circular plate, are made of aluminum. Material properties for aluminum and magnesium are shown in table 9 and table 10.

Table 9. Material properties for aluminum in ANSYS R18.1

Property	Value	Unit
Young´s modulus	$7.1*10^{10}$	[Pa]
Poisson's ratio	0.33	-
Bulk modulus	$6.9*10^{10}$	[Pa]
Shear modulus	$2.7*10^{10}$	[Pa]
Density	2770	$[\frac{kg}{m^3}]$

Table 10. Material properties for magnesium in ANSYS R18.1

Property	Value	Unit
Young´s modulus	$4.5*10^{10}$	[Pa]
Poisson's ratio	0.35	-
Bulk modulus	$5*10^{10}$	[Pa]
Shear modulus	$1.7*10^{10}$	[Pa]
Density	1800	$[\frac{kg}{m^3}]$

In this model a distributed mass was placed on the top of the sight as shown in the figure 27. This mass represents the robot tube and has a weight of 7 kg. Another mass, which is 90 kg represent human body and IFF. This distributed mass was applied to a stick at the stand and illustrated in figure 28. The problem investigation was considered when the missile leaves the robot tube. Note that the mass of the RBS 70 NG system is 45 kg.

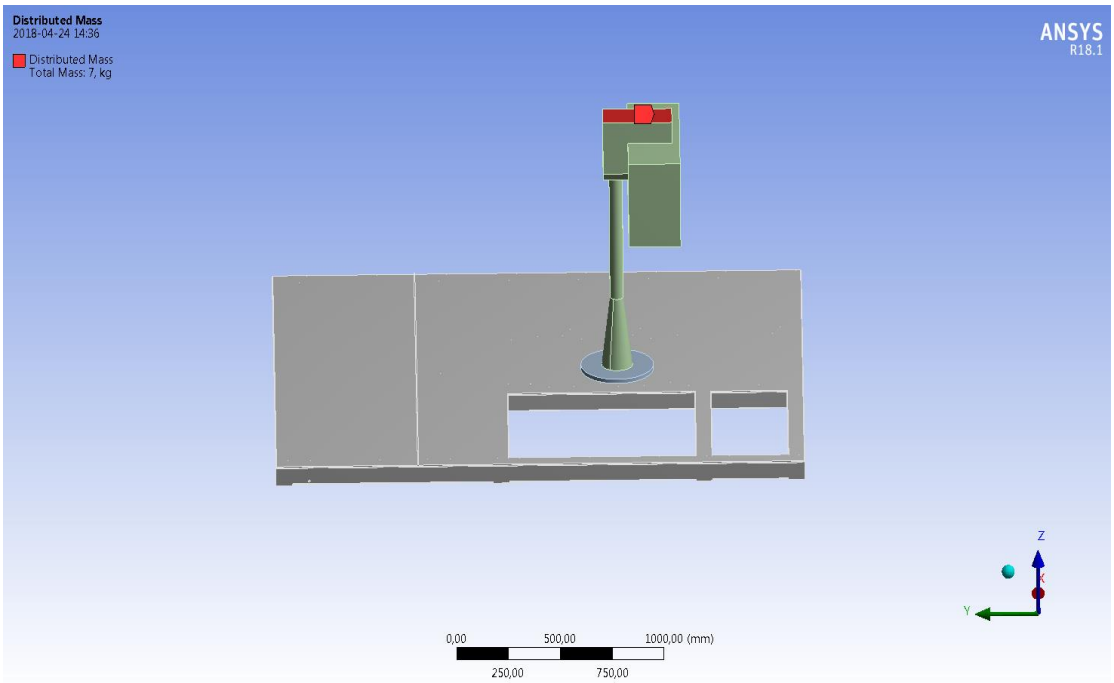

Figure 27. Distributed mass representing the robot tube (red spot).

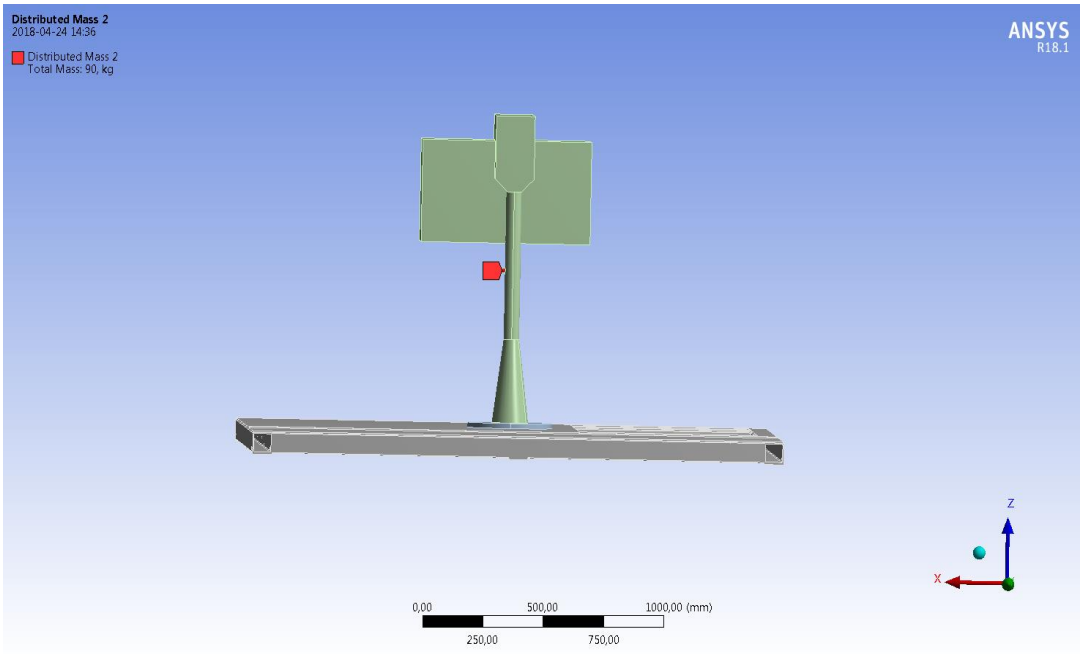

Figure 28. Distributed mass representing the human body and IFF (red spot).

Harmonic response requires modal analysis and the maximum mode number was set to 15 because this number of modes cover frequencies to 110 Hz.

The first constraint was applied at ten faces and is illustrated as yellow spots in Figure 29, which represent the vertical beams of the platform. The constraint was defined as displacement and set to zero in z direction. In x and y direction the displacement is set to free.

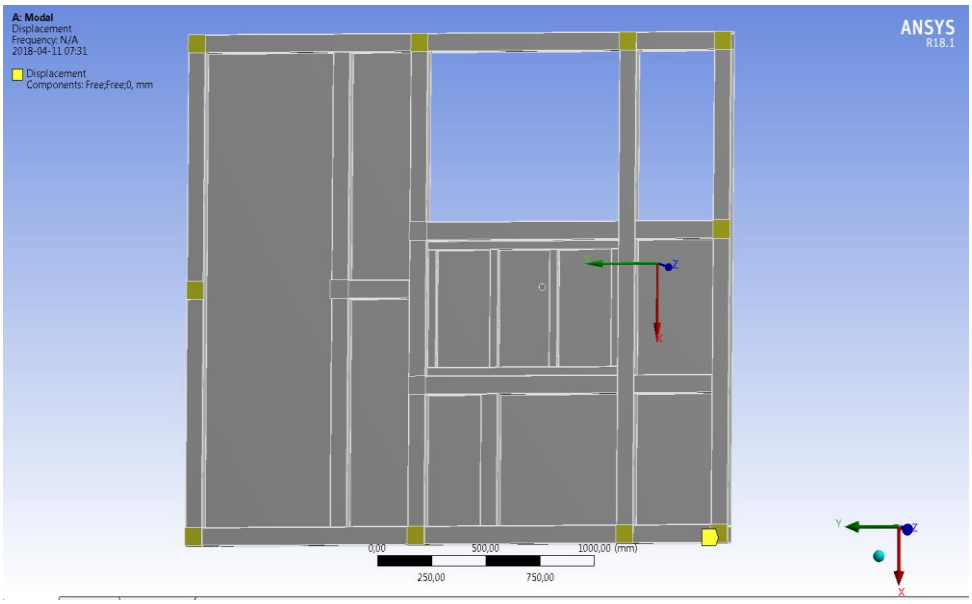

Figure 29. Constraint representing the vertical beams of the platform (yellow spots).

The second constraint was applied on two beams below the roof and the displacement was set to zero in z direction. In x and y direction the displacement was set to free. The constraint represents the vertical wall and this approach is illustrated as yellow spots in figure 30.

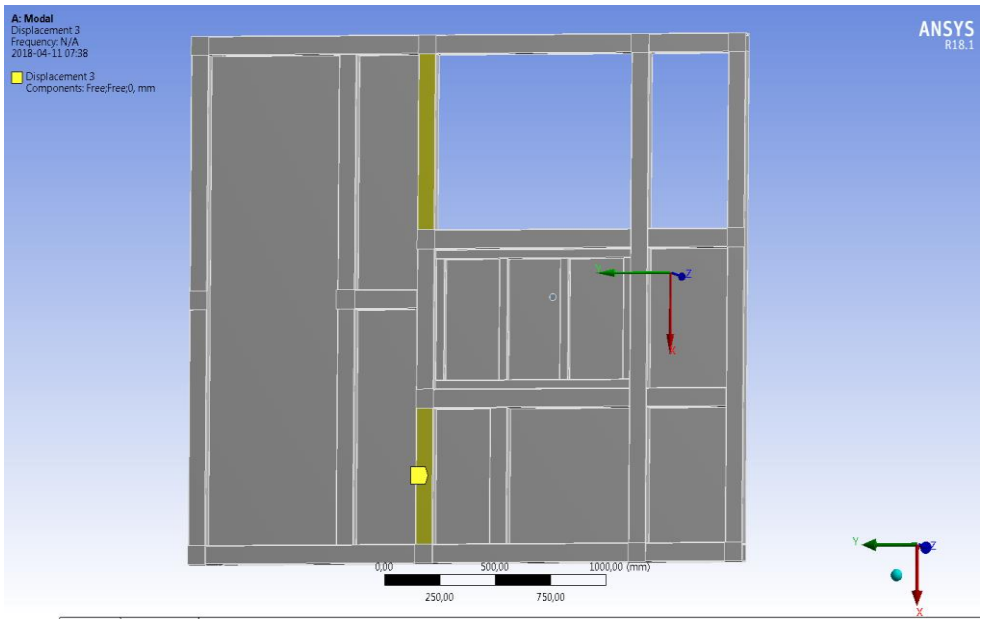

Figure 30. Constraint representing the two beams below the roof of the platform (yellow spots).

The last constraint was applied around the roof and the displacement was set to zero in x and y direction. The displacement is free in z direction and this approach is illustrated as yellow spots in figure 31.

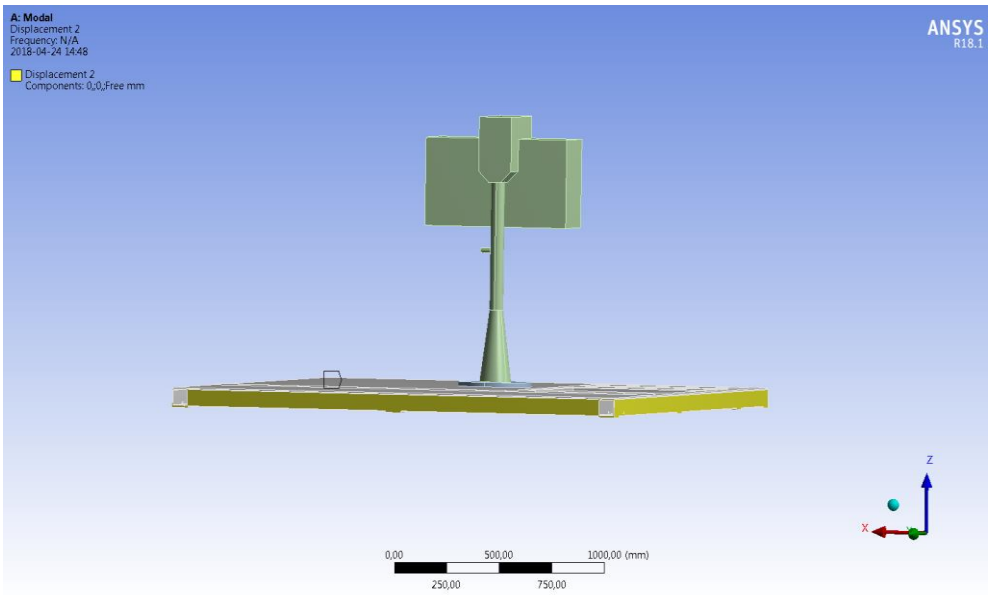

Figure 31. Constraint representing yellow spots around the roof of the platform.

Note that in figure 31 only two faces are visible, but additionally two faces which is symmetrically on the other side of the roof is constrained with this type of displacement.

Inertial acceleration is applied to study the harmonic response of the vehicle integrated system. Measured values from an accelerometer (acc4) in an experimental test where used as exciting acceleration on the roof of the weapon platform and inputted in ANSYS R18.1. Note that three other accelerometers in the experimental test were placed at the circular plate (acc3), stand (acc2) and sight (acc1). The placements of the accelerometers are illustrated in figure 32.

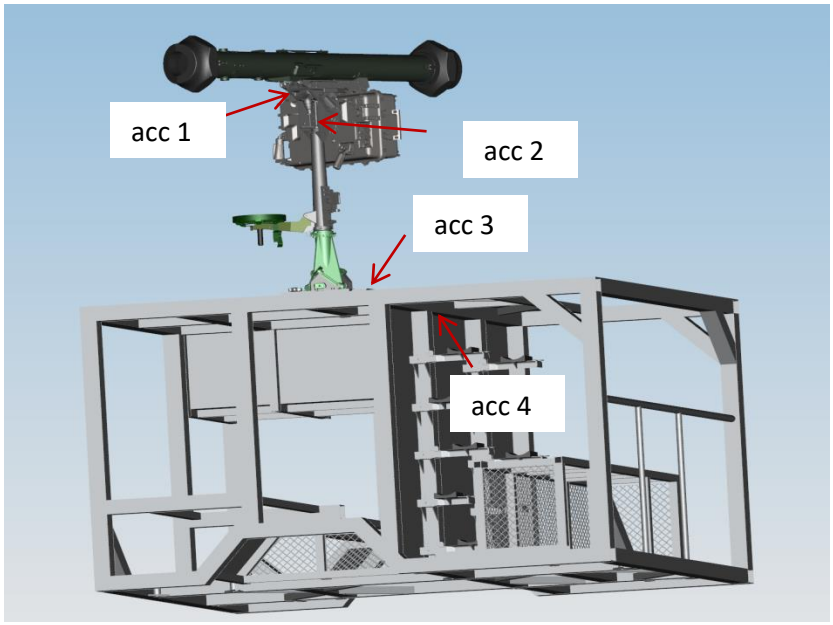

Figure 32. Placements of the four different accelerometers during the firing exercise.

The accelerometer was measuring the amplitude response over a period of time, so a fast Fourier transform was used in MATLAB R2015a to convert the amplitude response over the frequency spectrum (see table 11). Figure 33 illustrates the exciting acceleration over the frequency spectrum, made by inputting table 11 in ANSYS R18.1.

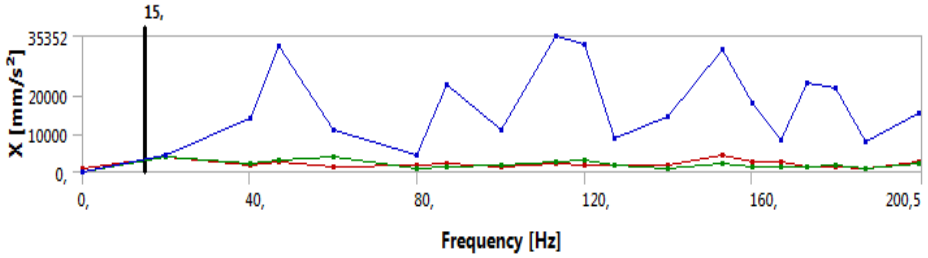

Figure 33. The exciting acceleration over the frequency spectrum.

Table 11. Values calculated by using fast Fourier transform in MATLAB R2015a in three different directions for acc4

Frequency [Hz]	Z direction [$\frac{mm}{s^2}$]	X direction [$\frac{mm}{s^2}$]	Y direction [$\frac{mm}{s^2}$]
0	0	982	0
20	4305	4084	3830
40	14003	1866	2072
47	32809	2750	2946
60	10782	1277	3830
80	4419	1866	786
87	22586	2160	1473
100	10802	1375	1823
113	35352	2023	2702
120	33093	1866	2946
127	8543	1571	1768
140	14239	1768	1080
153	32013	4419	2357
160	17961	2553	1485
167	8248	2455	1277
173	23175	1375	1401
180	21604	1178	1669
187	7856	1080	786
200	15427	2455	2259
207	19601	1178	2455

For the harmonic response it is useful to define the frequency range, which means that the solver will create an amplitude response up to 110 Hz in this case and the solution interval is set to 21. Some points of interest to study the harmonic response are illustrated in figure 34, 35 and 36.

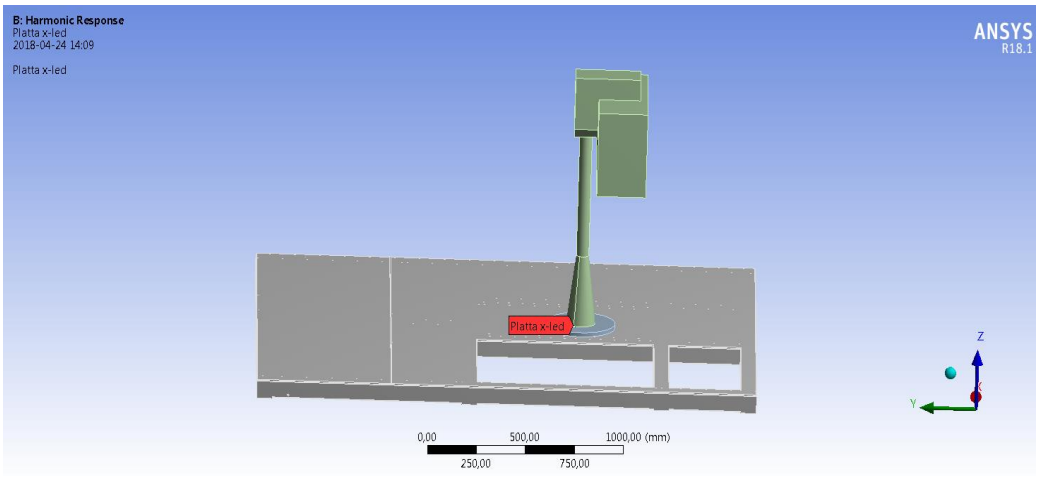

Figure 34. A point marked at the plate connecting RBS 70 NG system and the platform (point1).

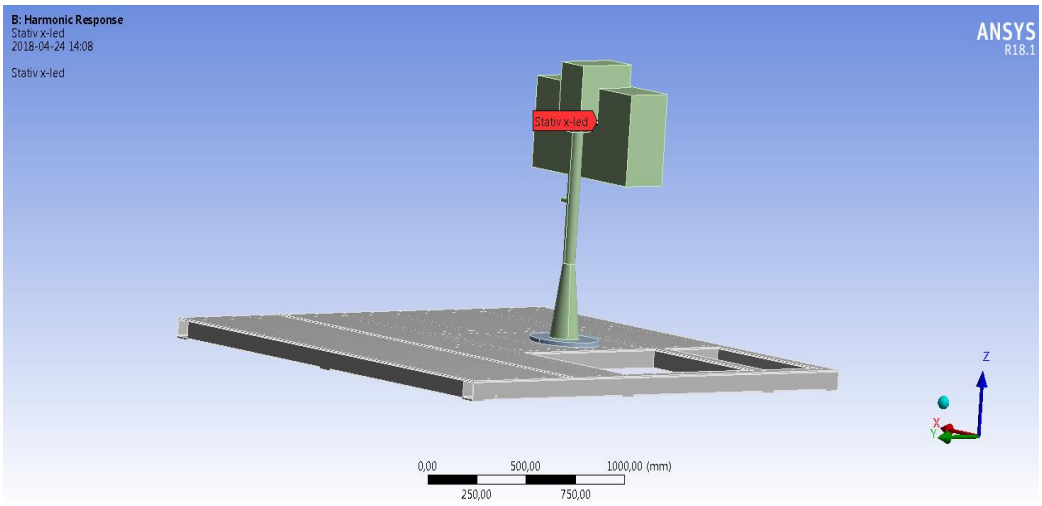

Figure 35. A point marked at the stand (point2).

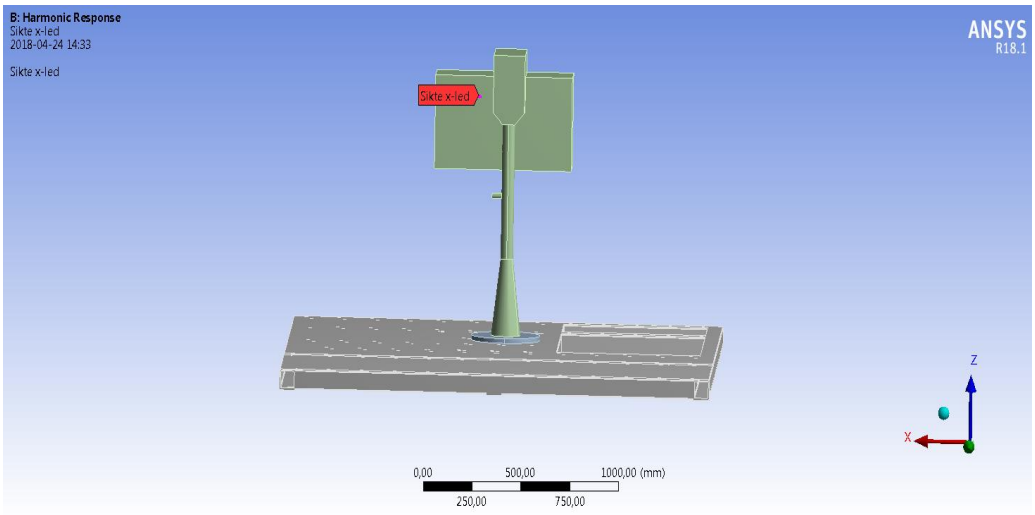

Figure 36. A point marked at the sight (point3).

The way to model RBS 70 NG on a thick and thin roof with dampers in ANSYS R18.1 is approximate the same as without dampers but with some additional steps. In the modal response it was necessary to set the function "damped" to yes and additionally change the solver type to reduce damped. The stiffness coefficient is also defined in this part of the project tree. Equation (23) describes the formula to calculate the stiffness coefficient [15].

$$\beta = \frac{2\zeta}{\omega_3 + \omega_4} \quad (23)$$

In this case the damping ratio, ζ is set to 0.04 for a rubber damper [7]. The frequency range $\omega_3 + \omega_4$ was set to 110 Hz because the gyro of the SMU has measurement frequency interval up to around 100 Hz. The value on β will result in 0.000533. Under connection in the project tree four dampers can be defined in the model by using the function bushing. The longitudinal damping coefficient for a natural rubber is 0.1 $\frac{\mathrm{Ns}}{\mathrm{mm}}$ [16]. As mentioned before values on stiffness in z direction can be chosen to 960 $\frac{\mathrm{N}}{\mathrm{mm}}$, 780 $\frac{\mathrm{N}}{\mathrm{mm}}$ and 640 $\frac{\mathrm{N}}{\mathrm{mm}}$, which also meet the requirement on 4-6 Hz in natural frequency for the vehicle integrated system. Values on stiffness in x and y direction is 165 $\frac{\mathrm{N}}{\mathrm{mm}}$ for the damper with 960 $\frac{\mathrm{N}}{\mathrm{mm}}$ in z direction, 125 $\frac{\mathrm{N}}{\mathrm{mm}}$ for the damper with 780 $\frac{\mathrm{N}}{\mathrm{mm}}$ in z direction and 107 $\frac{\mathrm{N}}{\mathrm{mm}}$ for the damper with 640 $\frac{\mathrm{N}}{\mathrm{mm}}$ in z direction. For the harmonic response it is necessary to define the constant damping value and for rubber the value is 0.04 as mentioned before.

5. RESULTS AND DISCUSSIONS

Experimental tests have been done to study the Power Spectral Density (PSD) for the system applied on the platform, which was named as reference configuration. PSD illustrates the strength of the energy as a function of frequency and has the unit $\frac{G^2}{Hz}$, where G is the acceleration measured in $\frac{mm}{s^2}$. One advantageous to study a squared signal frequency spectrum, is it results in a positive quantity and the mean value can be calculated [17]. Figure 37 illustrates PSD values measured by SMU gyro in elevation direction during experimental tests and it shows the strongest noise to be around 45 Hz.

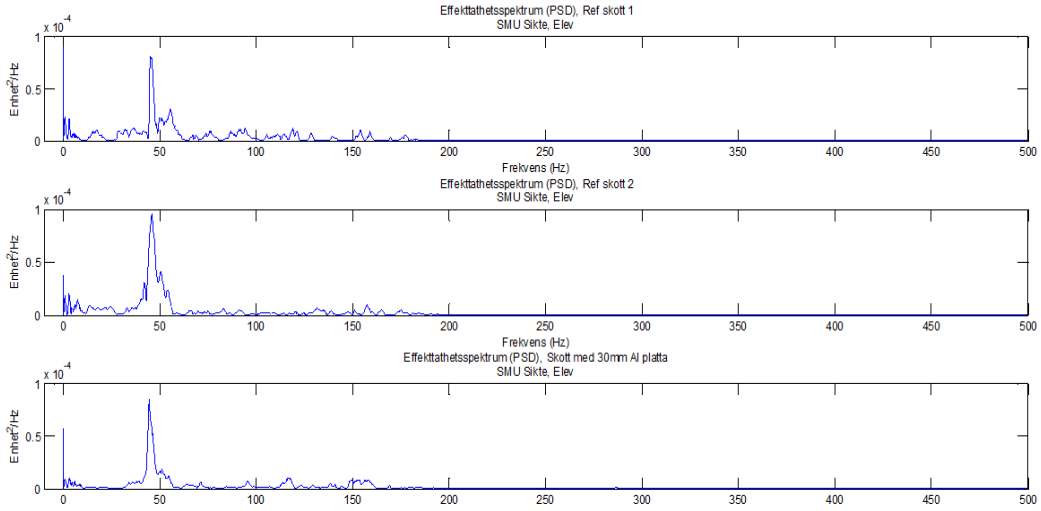

Figure 37. Measured PSD values in elevation direction by SMU.

Figure 38 illustrates PSD values measured by SMU gyro in azimuth direction during experimental tests and it shows the strongest noise to be around 110 Hz.

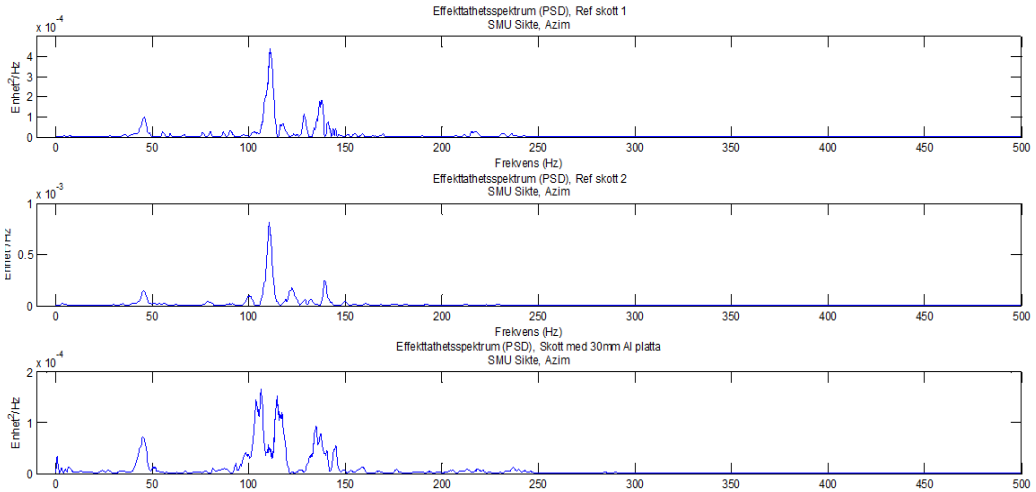

Figure 38. Measured PSD values in azimuth direction by SMU.

Among the 15 modes from the modal analysis performed on reference model it was detected 2 modes at 41 Hz and 96 Hz which can disturb SMU at the NG Sight in elevation direction and azimuth direction. These modes will be of interest to study for the harmonic response and are illustrated in figure 39 and 40.

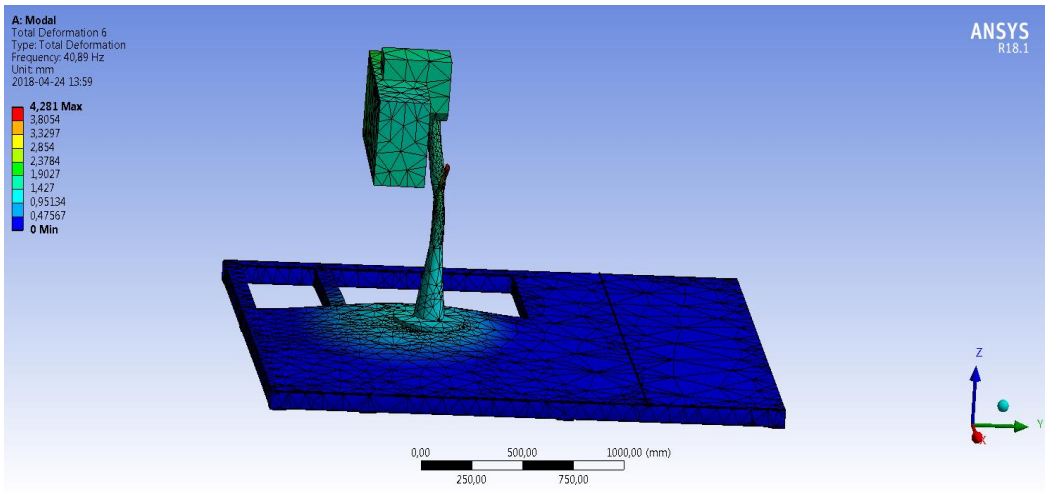

Figure 39. Mode shape at 41 Hz for the reference system.

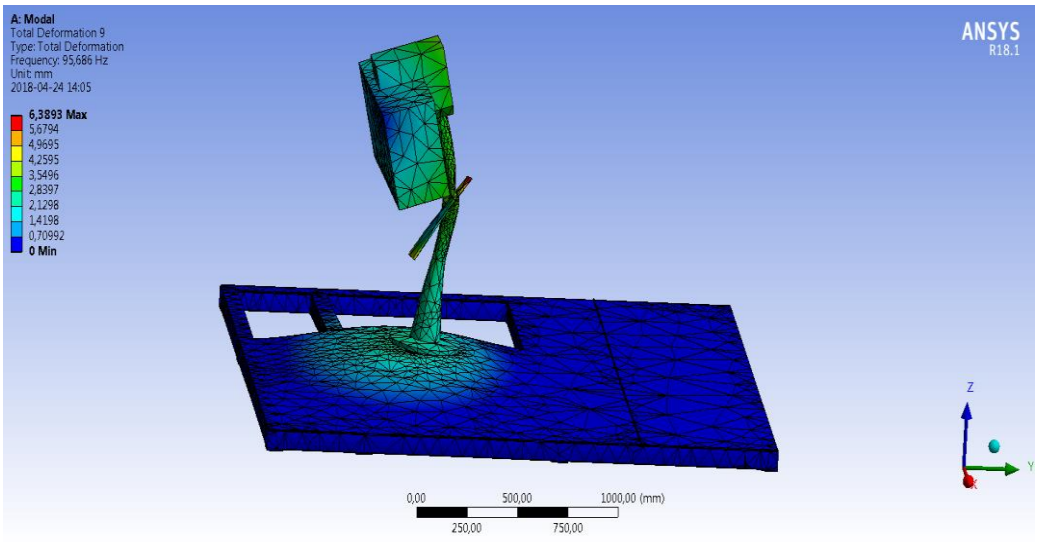

Figure 40. Mode shape at 96 Hz for the reference system.

The experimental data on the accelerometer (acc4) at the beam under the roof of the platform is defined as exciting acceleration on the roof of the platform in ANSYS R18.1 as mentioned before. It does not really reflect the reality but the relationship between different solutions is more interesting than the values of the upcoming amplitude response. Figures 41, 42 and 43 illustrate the upcoming amplitude response in point1 (placed on interface plate between RBS 70 NG System and platform roof) for a solution with thin and thick plate without dampers.

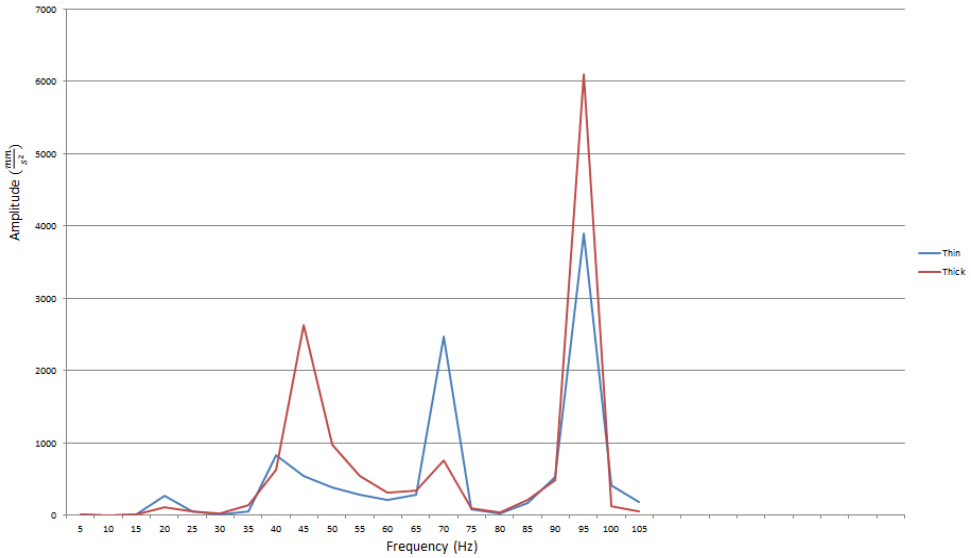

Figure 41. Amplitude response at point1 in x direction for thin plate and thick plate.

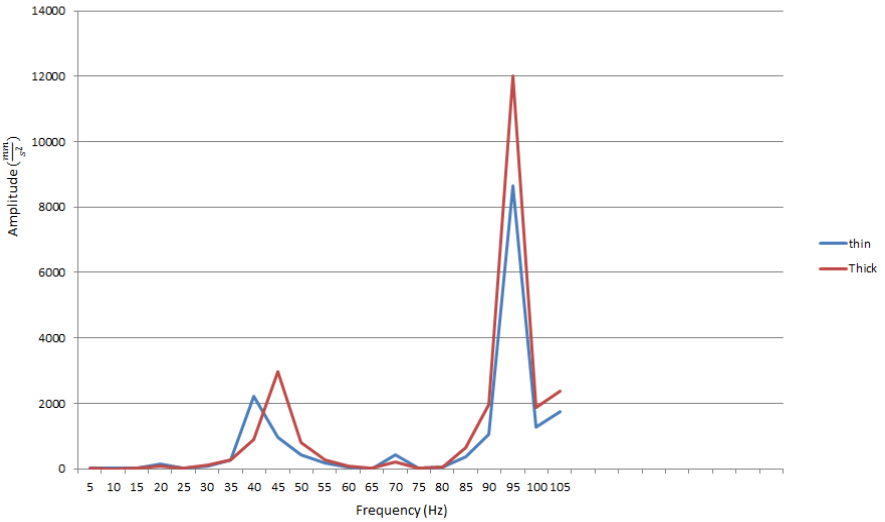

Figure 42. Amplitude response at point1 in y direction for thin plate and thick plate.

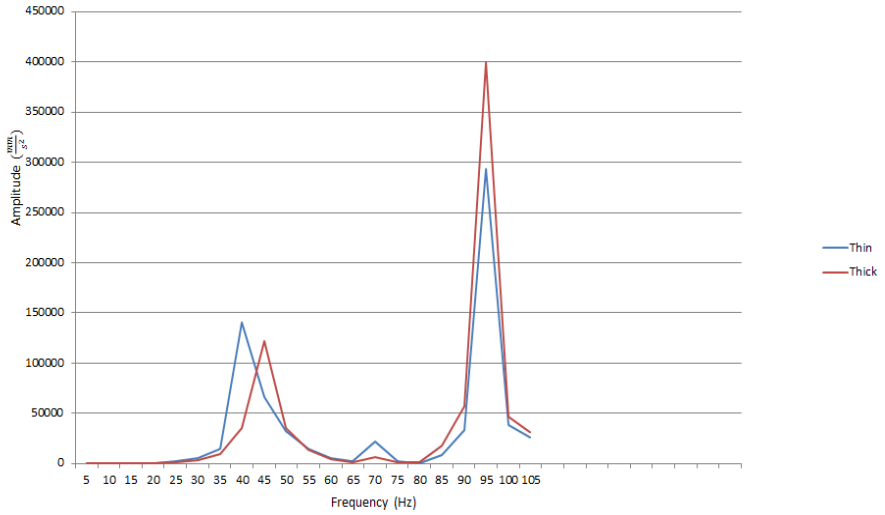

Figure 43. Amplitude response at point1 in z direction for thin plate and thick plate.

Figures 41, 42 and 43 illustrate two dominating peaks at around 42 Hz and 95 Hz. In PSD diagrams from experimental test illustrated in figure 37 and 38 two peaks can be detected for same frequencies. The mode shape at 41 Hz is illustrated in figure 39 and the mode shape at 95 Hz is illustrated in figure 40. The lower peak at 70 Hz is not relevant because this mode shape and frequency doesn't affect the SMU which was shown in the PSD diagrams. The mode shape is illustrated in figure 44.

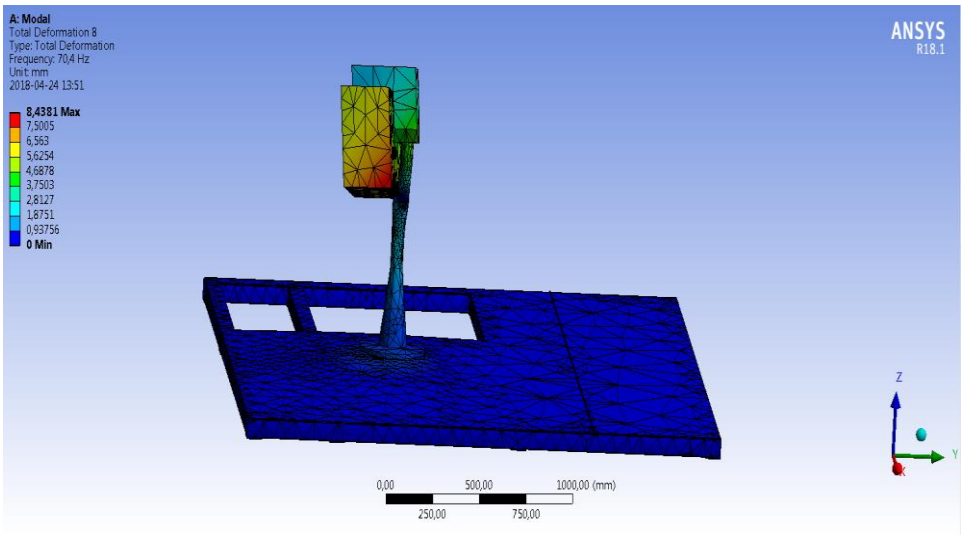

Figure 44. Mode shape at 70 Hz for the reference system.

Figures 45, 46 and 47 illustrate the upcoming amplitude response in point2 (placed on the NG Stand) for solution with thin and thick plate without dampers.

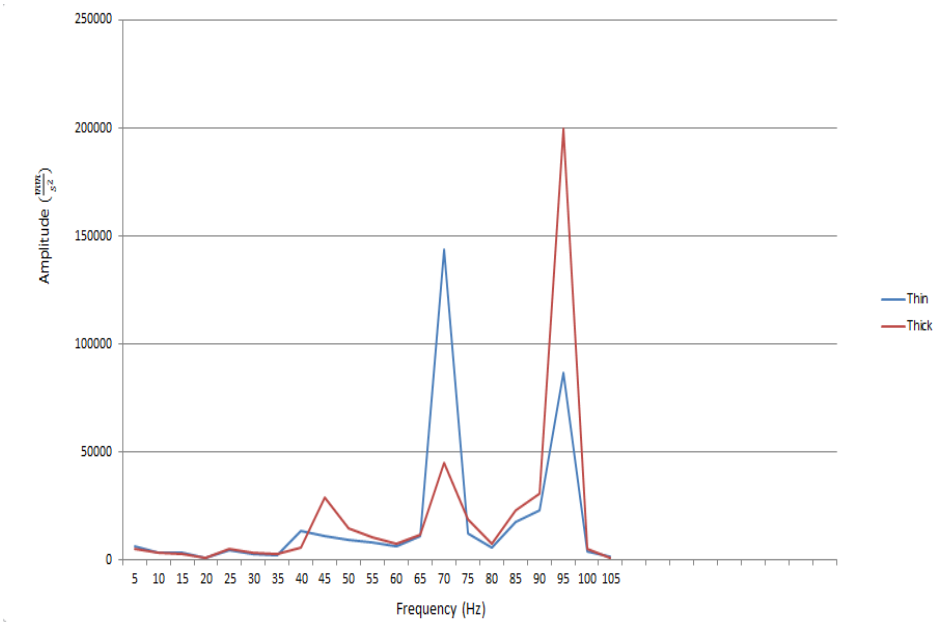

Figure 45. Amplitude response at point2 in x direction for thin plate and thick plate.

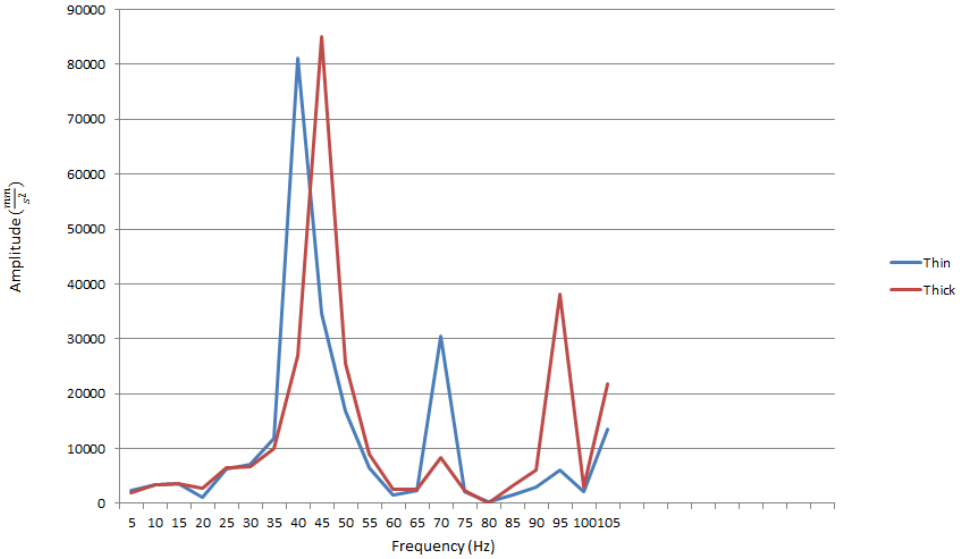

Figure 46. Amplitude response at point2 in y direction for thin plate and thick plate.

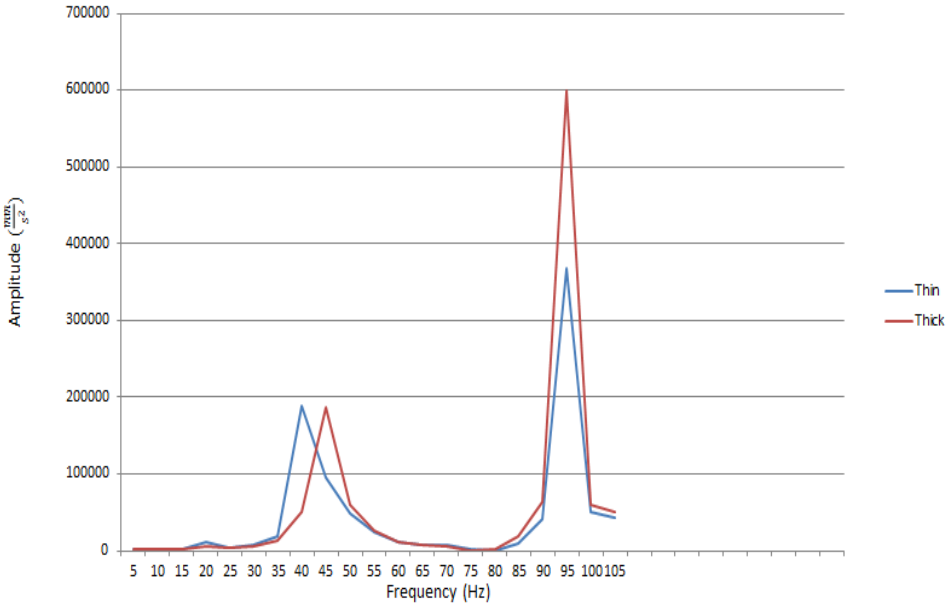

Figure 47. Amplitude response at point2 in z direction for thin plate and thick plate.

The point2, which is placed at the stand has stronger peaks comparing to point1, but the peak at 70 Hz in z direction is very low and much higher in x direction for point2.

Figures 48, 49 and 50 illustrate the upcoming amplitude response in point3 (placed on the NG Sight) for solution with thin and thick plate without dampers.

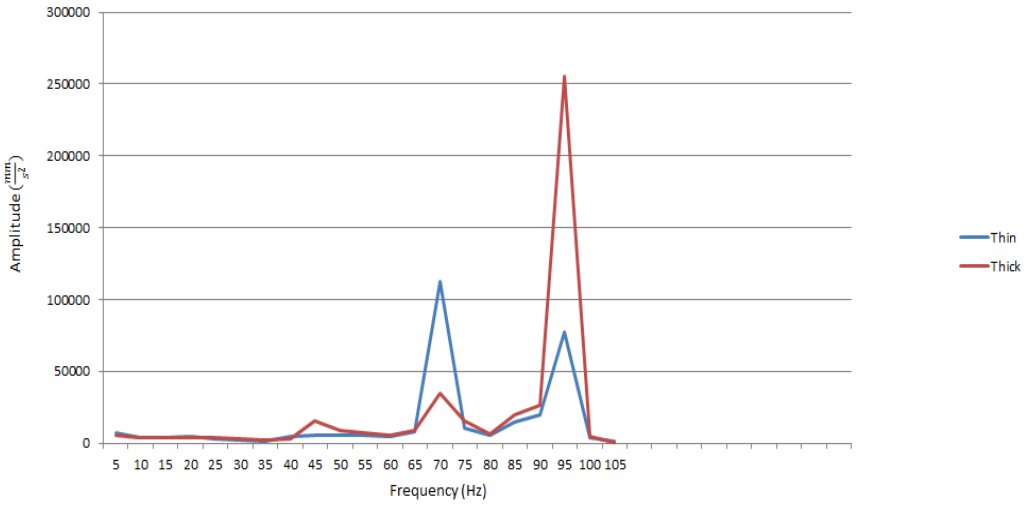

Figure 48. Amplitude response at point3 in x direction for thin plate and thick plate.

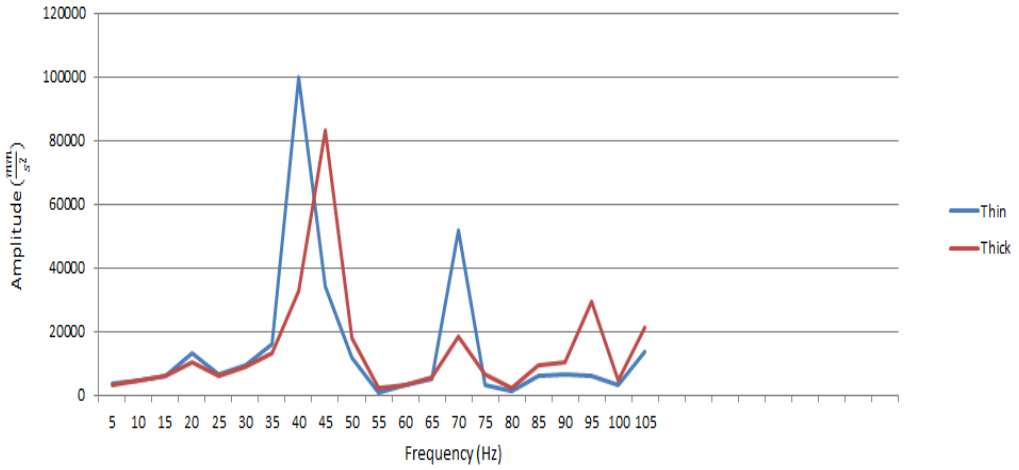

Figure 49. Amplitude response at point3 in y direction for thin plate and thick plate.

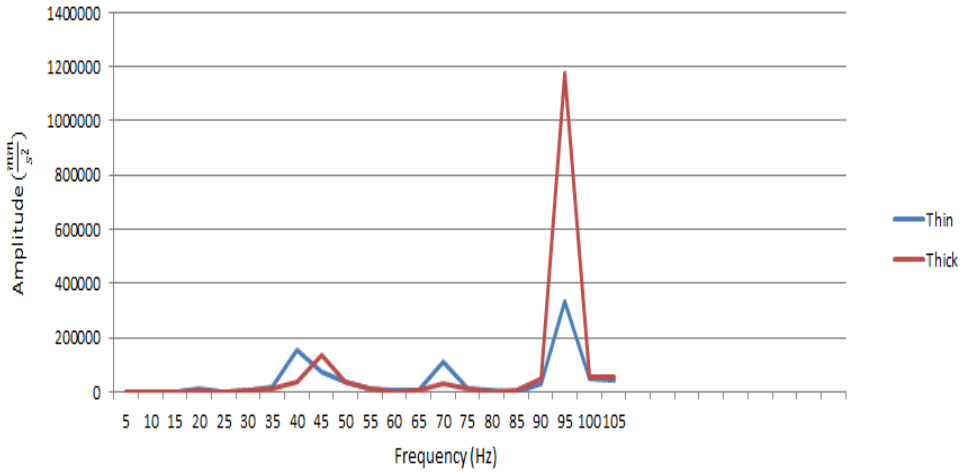

Figure 50. Amplitude response at point3 in z direction for thin plate and thick plate.

By studying z direction for point1, point2 and point3 it shows that a solution with thick plate is a better choice concerning disturbance of the system in elevation direction than using a thin plate, but in azimuth direction it is on the contrary. It is not big difference between thin and thick plate regarding amplitude level. Modification with thick plate was not giving satisfying results, because the thick plate is placed on small area on the roof and didn't contribute to stiffer structure. It just increases the mass on the beam below. It is necessary to extend the thick plate all the way in width direction, but it is not possible because of the weight requirements and limitation regarding placement of the compartment on the roof.

By analyzing the figure 40, it is illustrated that the mode shape is bended around x axis and this may be because the stand is too weak. This weakness may be a reason to the strong peak at 95 Hz in the diagrams. Without construction changes this problem with bending can be tested by input an extra constraint in ANSYS R18.1 and make the stand stiffer. The constraint was applied around the stand where the displacement was set to zero in x and y direction. The displacement is free in z direction and this approach is illustrated as yellow spot in figure 51.

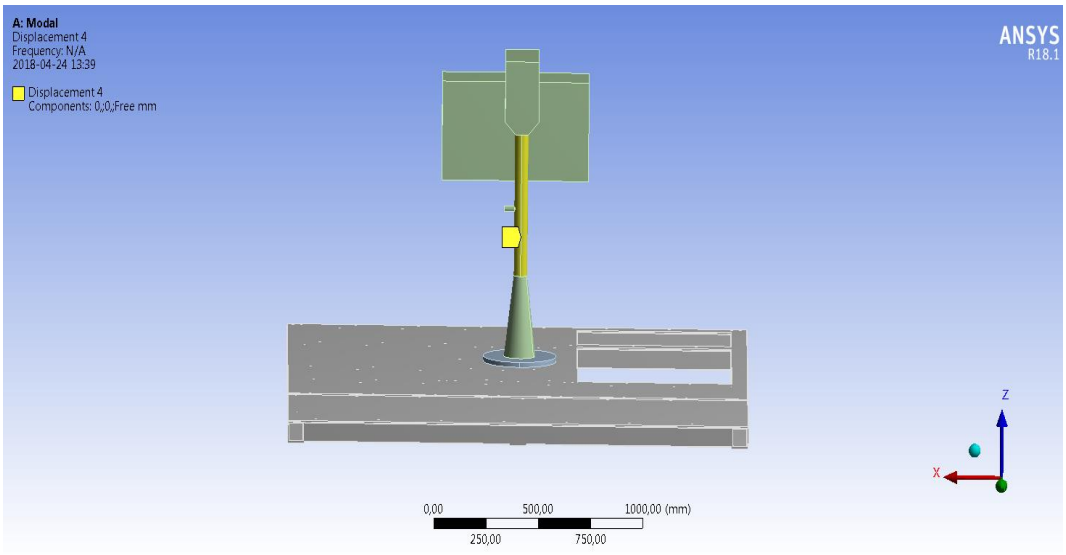

Figure 51. Constraint applied around the stand (yellow spots).

The upcoming amplitude response from ANSYS R18.1 at the sight in z direction is illustrated in figure 52.

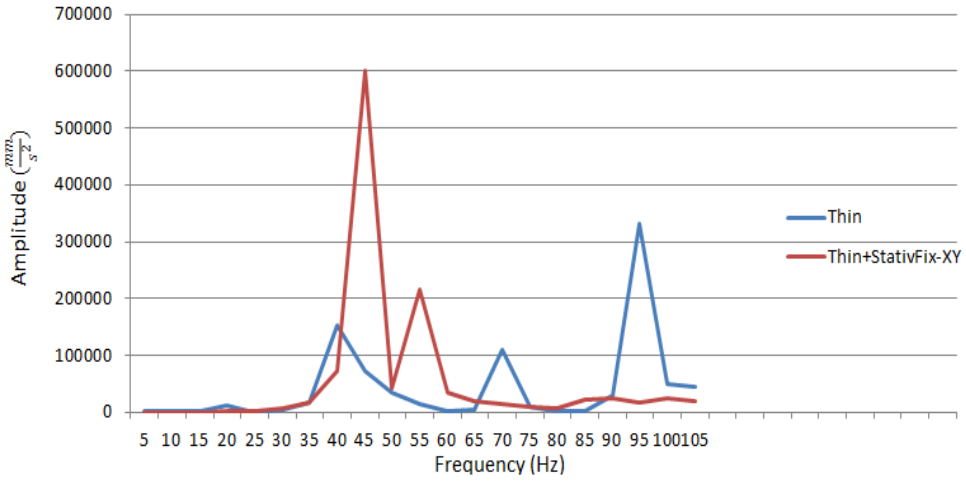

Figure 52. Amplitude response in z direction at the sight for thin plate and thin plate with constrained stand.

Figure 52 illustrates two dominating peaks at around 45 Hz ad 55 Hz for a solution with thin plate and constrained stand. The mode shape at 45 Hz is illustrated in figure 53 and the mode shape at 55 Hz is illustrated in figure 54.

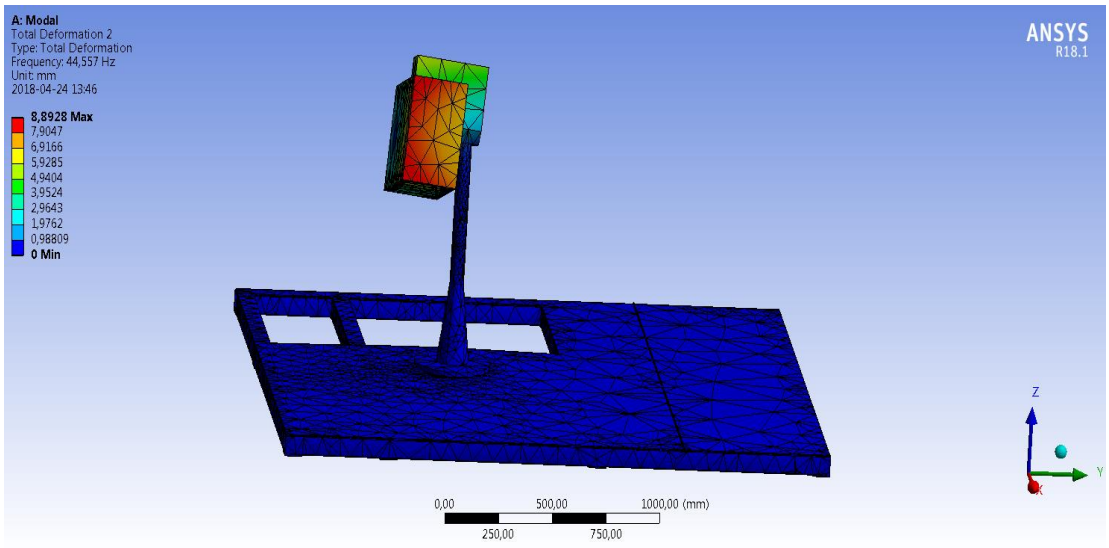

Figure 53. Mode shape at 45 Hz for the thin plate with constrained stand.

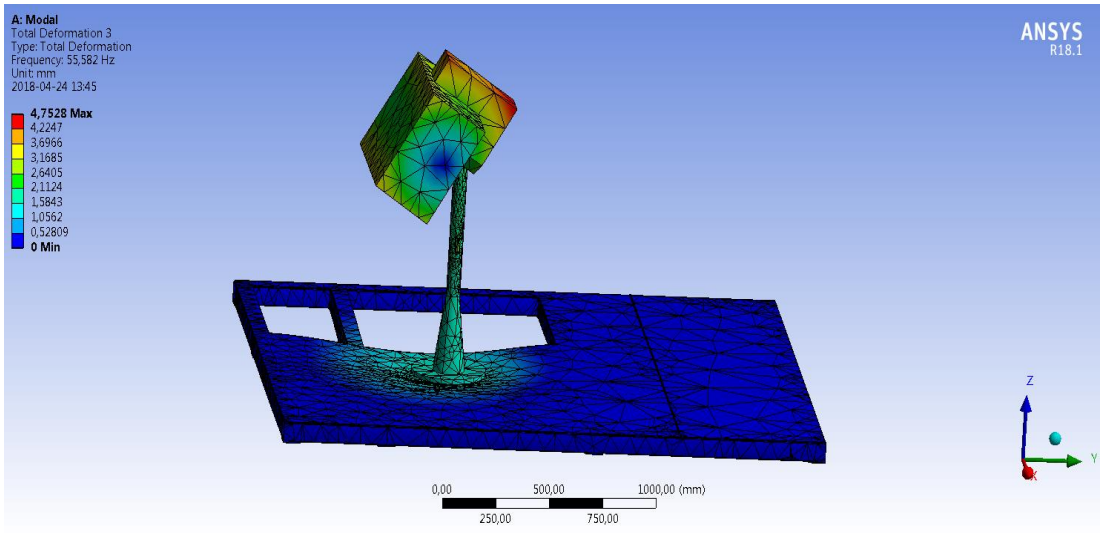

Figure 54. Mode shape at 55 Hz for the thin plate with constrained stand.

The mode shape at 45 Hz in figure 53 affects the movement of the SMU in azimuth direction similar as the mode shape at 95 Hz without constraint around the stand. By stiffening the stand the amplitude will be amplified at lower frequency. The reason may be that the magnification ratio have been reduced, because of excitation frequency is farther away from the resonance of SMU. The mode shape at 55 Hz in figure 54 affects the movement of the SMU in elevation direction similar as the mode shape in figure 39.

By introducing dampers to the interface between RBS 70 NG system and the platform, the amplitude response will be different compared to the cases mentioned with unconstrained NG stand. Figures 55, 56 and 57 illustrate the comparison in upcoming amplitude response at point1 for a solution with thin and thick plate with dampers as well as without dampers.

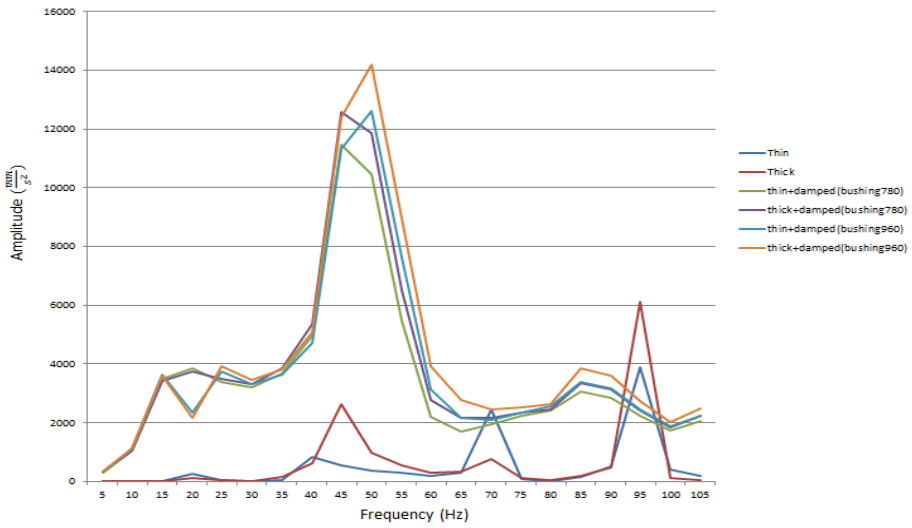

Figure 55. Amplitude response at point1 in x direction for concept a,b,c and reference model.

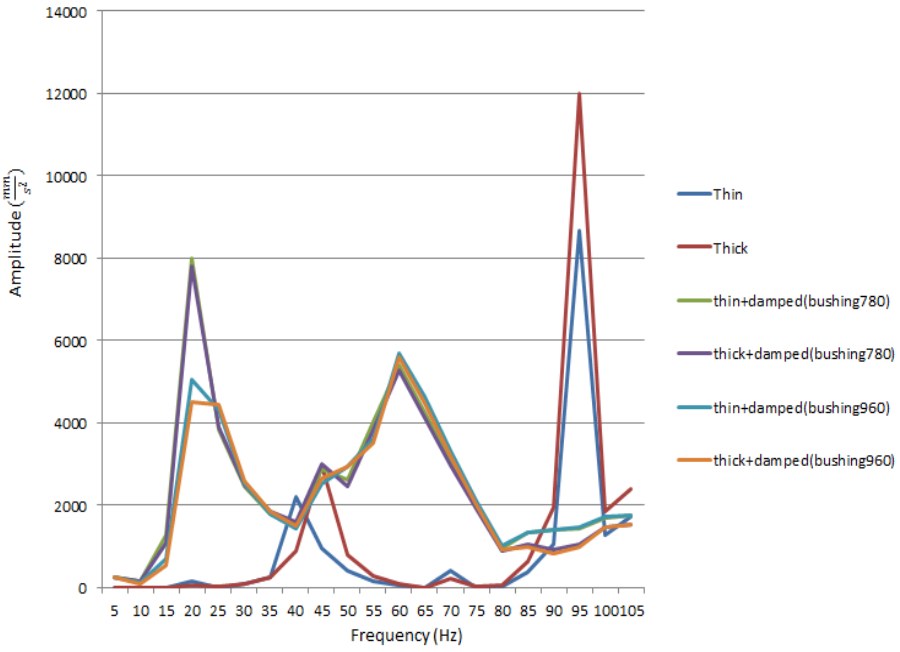

Figure 56. Amplitude response at point1 in y direction for concept a,b,c and reference model.

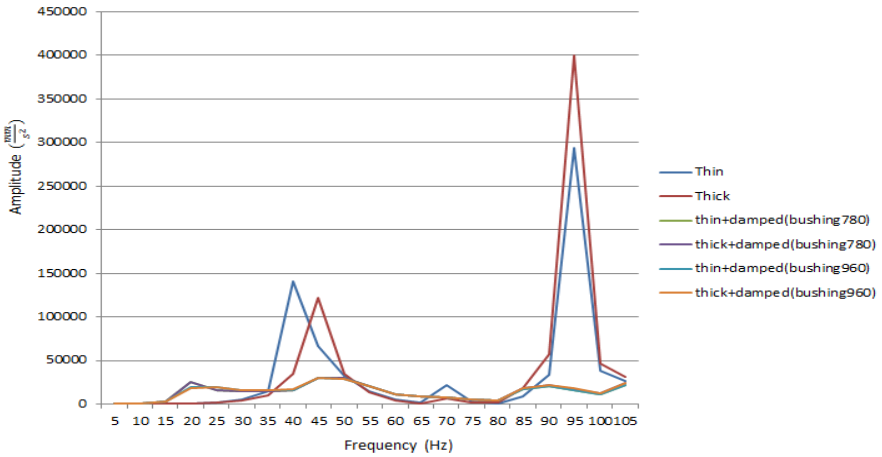

Figure 57. Amplitude response at point1 in z direction for concept a,b,c and reference model.

The mode shape at 20 Hz for a solution with thin plate plus dampers is illustrated in figure 58.

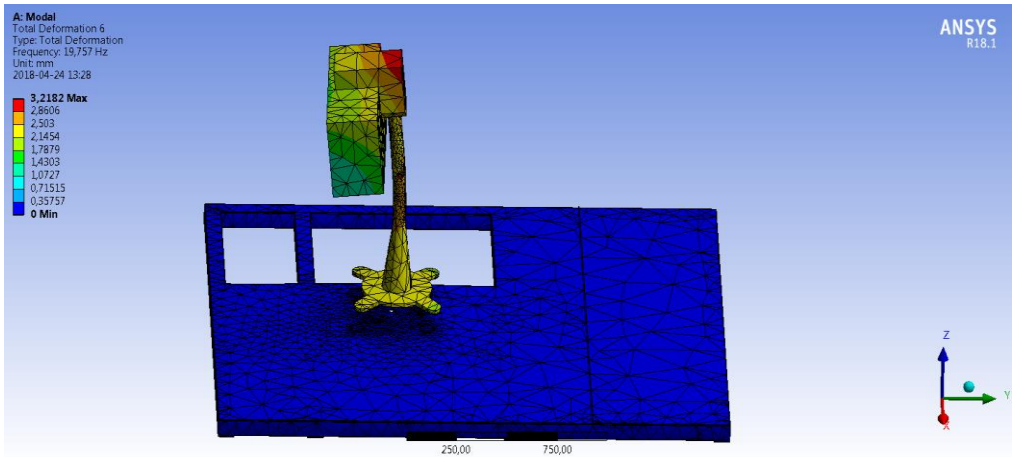

Figure 58. Mode shape at 20 Hz for the thin plate connected with dampers of stiffness value 780 $\frac{N}{mm}$.

The mode shape in figure 58 affects the movement of the SMU in elevation direction similar as the mode shape in figure 39. This may be as mentioned before that the magnification ratio has been reduced, because of excitation frequency is farther away from the resonance of SMU. The upcoming strong peaks for the plate at the interface between RBS 70 NG and the platform roof in x and y direction may be because of dampers are much weaker in these directions compared with z direction. The stiffness in z direction is six times greater compared to the stiffness in x and y direction. The mode shape at 86 Hz is illustrated in figure 59.

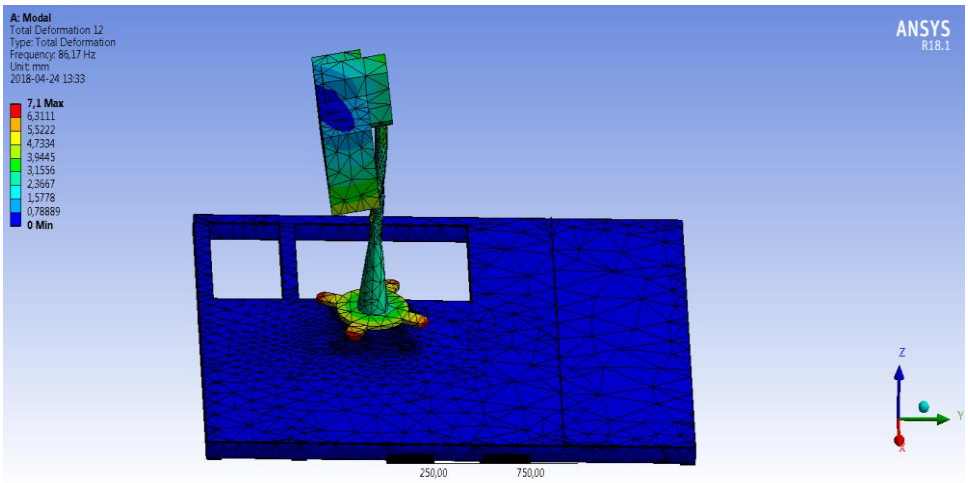

Figure 59. Mode shape at 86 Hz for the thin plate connected with dampers of stiffness value 780 $\frac{N}{mm}$.

The mode shape in figure 59 affects the movement of the SMU in azimuth direction similar as the mode shape in figure 40. In the case without dampers the roof of the platform is deforming and the case with dampers the dampers is deforming. This may be a reason why the similar mode shape has different natural frequency. The magnification ratio has been reduced, because of excitation frequency is farther away from the resonance of SMU.
Figures 60, 61 and 62 illustrate the comparison in upcoming amplitude response at point2 for a solution with thin and thick plate with dampers as well as without dampers.

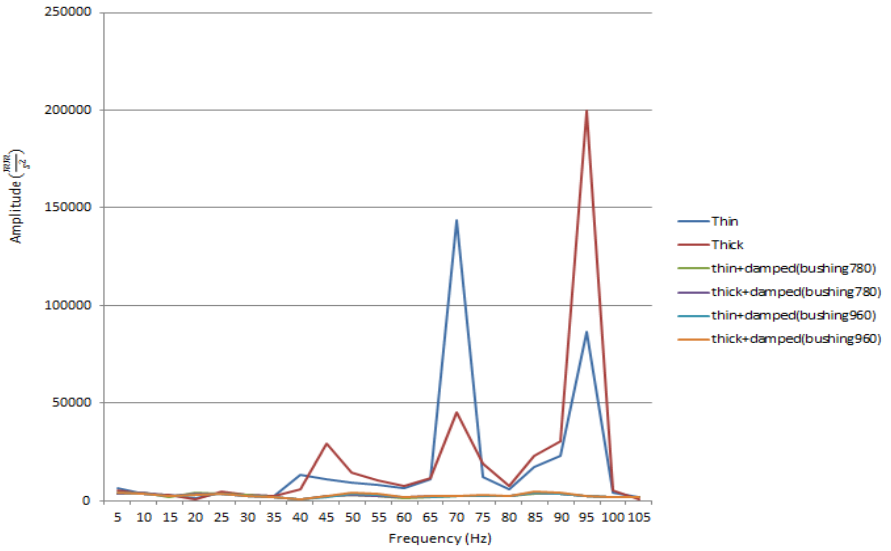

Figure 60. Amplitude response at point2 in x direction for concept a,b,c and reference model.

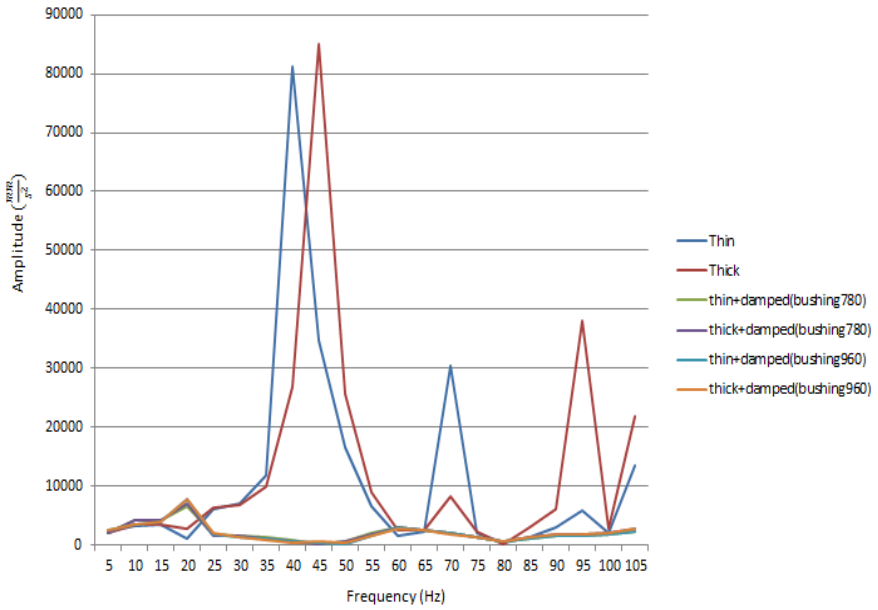

Figure 61. Amplitude response at point2 in y direction for concept a,b,c and reference model.

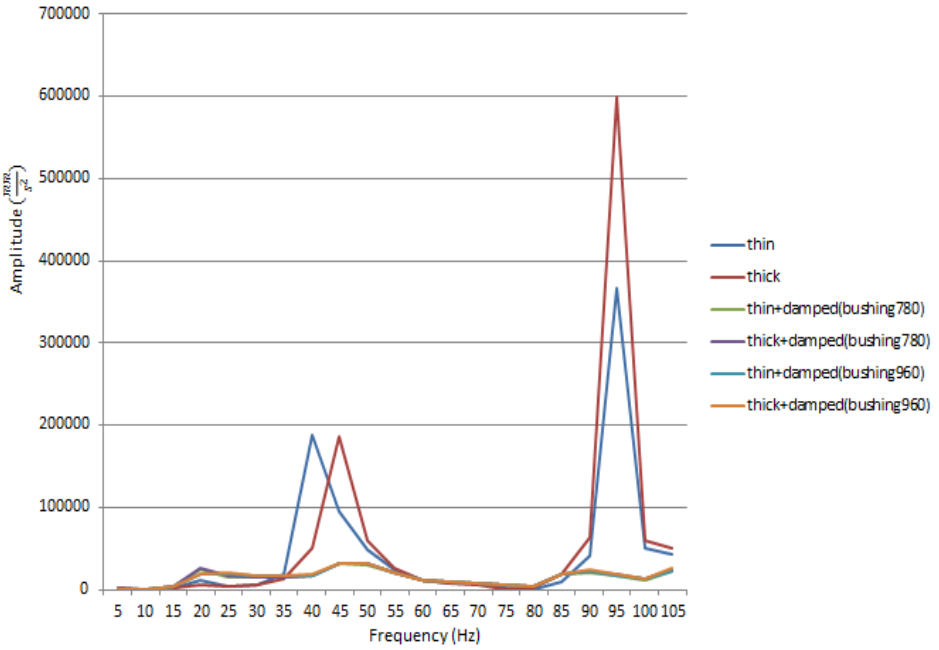

Figure 62. Amplitude response at point2 in z direction for concept a,b,c and reference model.

It is clearly illustrated that the amplitude response in all direction for the stand is reduced over the whole frequency spectrum. Figures 63, 64 and 65 illustrate the comparison in upcoming amplitude response at point3 for a solution with thin and thick plate with dampers as well as without dampers.

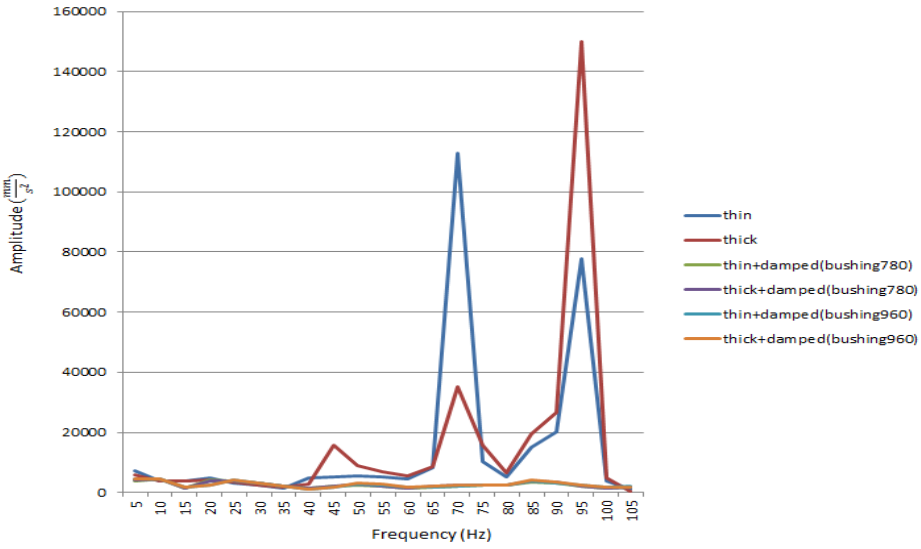

Figure 63. Amplitude response at point3 in x direction for concept a,b,c and reference model.

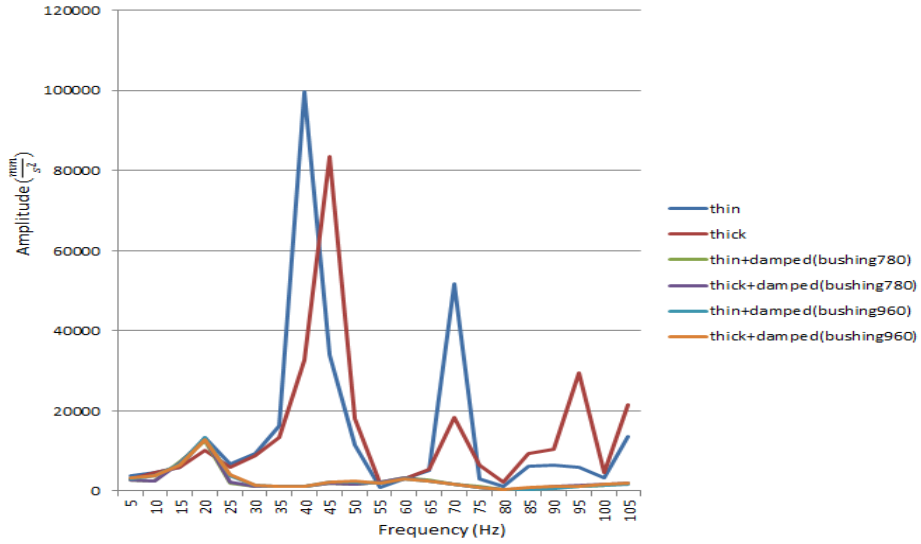

Figure 64. Amplitude response at point3 in y direction for concept a,b,c and reference model.

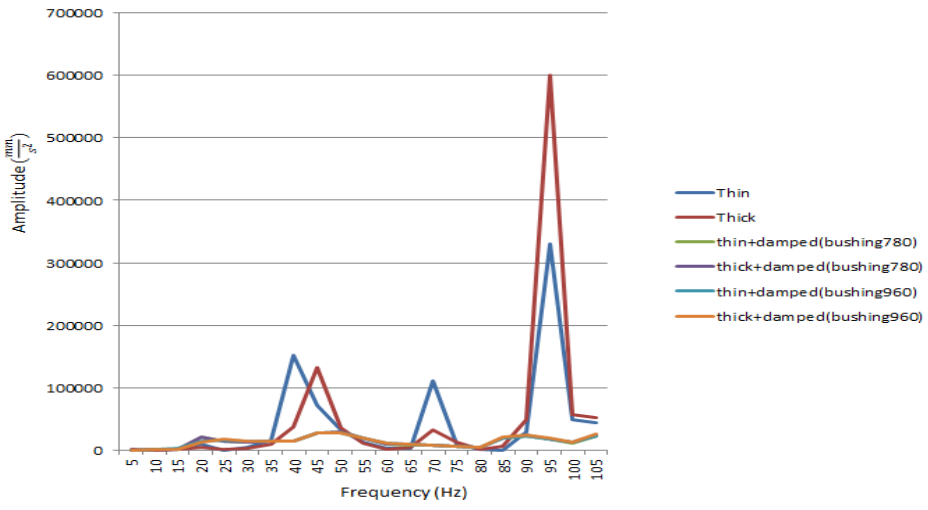

Figure 65. Amplitude response at point3 in z direction for concept a,b,c and reference model.

It is clearly illustrated that the amplitude response in all direction for the sight is reduced over the whole frequency spectrum. By changing the stiffness of the dampers, the amplitude response will change over the frequency spectrum and this is illustrated in figure 66. The damping value is the same for all three cases, which is as mentioned before 0.1 $\frac{\mathbf{N}}{\mathbf{mm}}$.

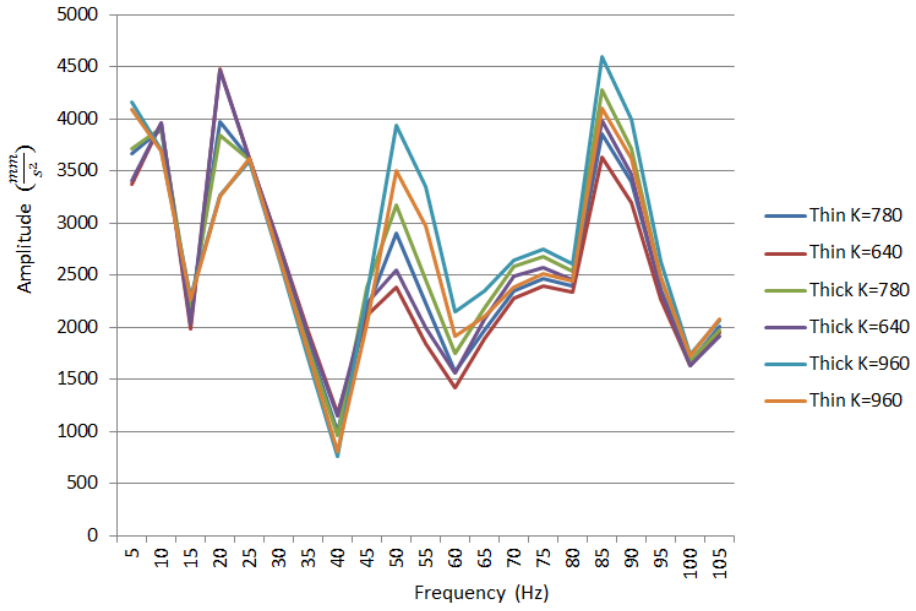

Figure 66. Amplitude response for the three different of stiffness values (640 $\frac{\mathbf{N}}{\mathbf{mm}}$, 780 $\frac{\mathbf{N}}{\mathbf{mm}}$ and 960 $\frac{\mathbf{N}}{\mathbf{mm}}$) for the dampers.

Figure 66 shows that the solution with dampers of stiffness value 640 $\frac{\mathrm{N}}{\mathrm{mm}}$ have lowest amplitude response for the frequencies around 95 Hz. To understand this amplitude response of different stiffness values on dampers it is useful to introduce the work formula [18];

$Q = F * s$ (24).

A softer damper (640 $\frac{\mathrm{N}}{\mathrm{mm}}$) compared to a harder damper (960 $\frac{\mathrm{N}}{\mathrm{mm}}$) has a greater measure of energy transfer because the deformation (distance s) of the dampers is greater i.e. more energy losses which transforms in heat. It is considered that the external force is the same for both dampers.

The natural frequency of the mode shape concerning to RBS 70 NG system requirements will be lower than 4-6 Hz, if the dampers have a stiffness value of 640 $\frac{\mathrm{N}}{\mathrm{mm}}$ and the distance between the dampers are 350 mm. The natural frequency of this case was calculated to 3.28 Hz and illustrated in figure 67.

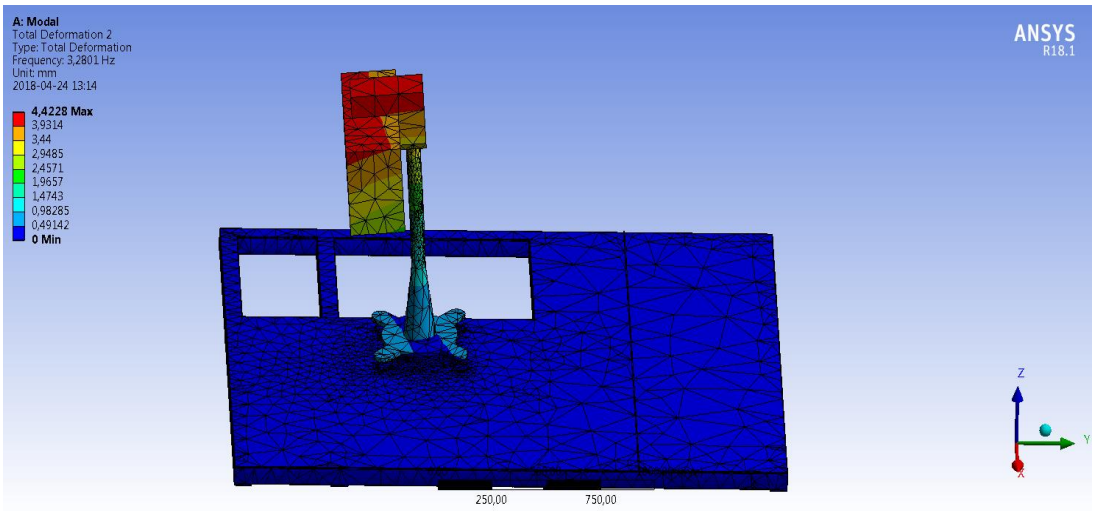

Figure 67. RBS 70 NG connected with dampers of stiffness value 640 $\frac{N}{mm}$ on a 5 mm thick plate.

One way to increase the natural frequency is to increase the distance between the dampers, but that is not possible because the space on the roof of the platform is limited. The solution will be to increase the stiffness of dampers and keep the distance between the dampers to 350 mm. A stiffness value of 780 $\frac{N}{mm}$ will result in a natural frequency of 3.48 Hz and this is illustrated in figure 68.

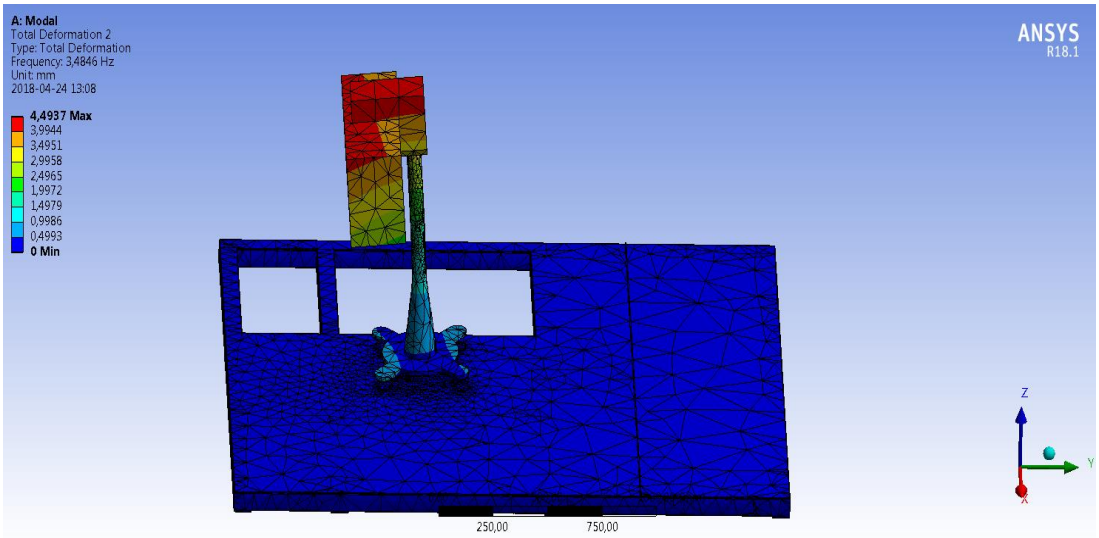

Figure 68. RBS 70 NG connected with dampers of stiffness value 780 $\frac{N}{mm}$ on a 5 mm thick plate.

By increasing the stiffness value from 780 $\frac{N}{mm}$ to 960 $\frac{N}{mm}$ it will result in a natural frequency of 3.7 Hz and this is illustrated in figure 69.

Dampers with stiffness value of 780 $\frac{N}{mm}$ or 960 $\frac{N}{mm}$ will fulfill the requirement for natural frequency in launching direction in according to investigation which has been performed for the RBS 70 NG system integrated on vehicle. The lower required limit on natural frequency was reduced to 3.5 Hz as mentioned before.

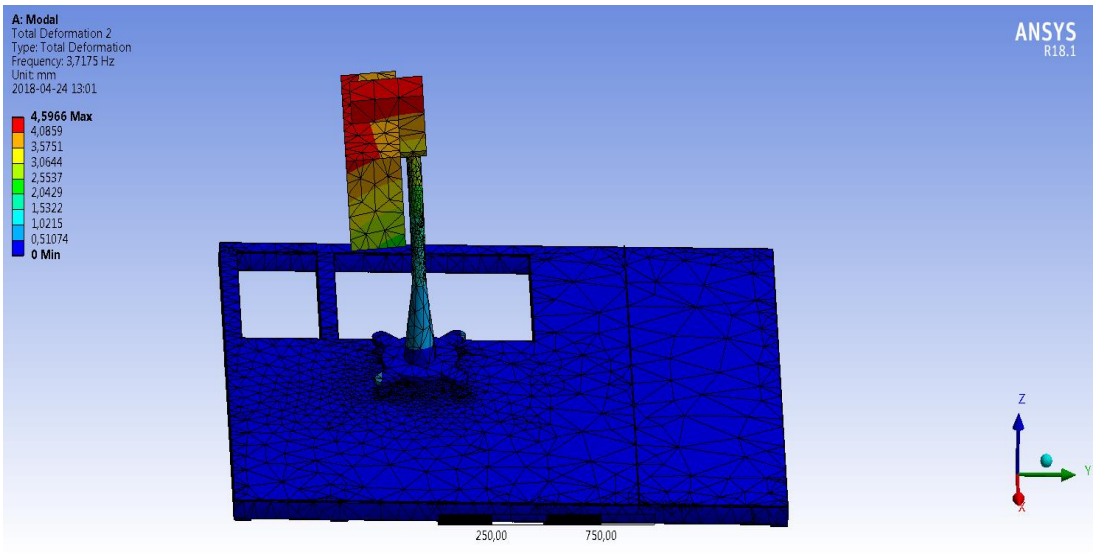

Figure 69. RBS 70 NG connected with dampers of stiffness value 960 $\frac{\mathbf{N}}{\mathbf{mm}}$ on a 5 mm thick plate.

6. CONCLUSION

Vehicle integrated RBS 70 NG system consists of an existing MANPADS configuration without legs mounted on a weapon platform which is placed on the vehicle. Disturbance may occur during firing and investigation should propose alternative solutions to reduce disturbance.

Power Spectral Density (PSD) measured during experimental test on the reference concept (original weapon platform) shows strongest level of the noise at 45 Hz in elevation direction and 110 Hz in azimuth direction. Three different concepts were investigated for the mechanical interface between RBS 70 NG system and weapon platform, which was also compared with the reference concept. The aim of the evaluation was to decrease the upcoming amplitude at 45 Hz and 110 Hz. The idea for the three proposal solution was to implement a stiff thick plate and dampers.

On the other hand a stiffer stand leads to a reduced amplitude response around 100 Hz which can cause disturbance of the SMU in azimuth direction, but the problem remains in elevation direction.

Dampers absorb energy and reduce the amplitude response across the entire frequency spectrum. It will give an advantageous if the distance between dampers increases as much as possible to reduce the stiffness of the dampers and meet requirements regarding natural frequency of the 3.5(4)-6 Hz. Less stiff dampers cause less disturbance of the system. Due to design limitations, the distance between the dampers must be less than for the legs of MANPADS and for the existing design it is stated to be 350 mm. The thicker plate doesn't help to minimize the amplitude response as dampers do. Proposed design for the interface between RBS 70 NG and platform will be a 15 mm plate in order to screw the damper more easily at the interface and the stiffness value of the dampers is chosen to 780 $\frac{\mathrm{N}}{\mathrm{mm}}$, because it fulfills the requirement of natural frequency and also have lower upcoming amplitude response compared to the solution of a stiffness value of 960 $\frac{\mathrm{N}}{\mathrm{mm}}$.

7. FUTURE WORK

The results from ANSYS R18.1 should be verified by performing experimental tests because the RBS 70 NG system was modeled as a simplified model. Calculating in for example ABAQUS would have been a good idea for comparing and analyzing which program is best suited for such frequency calculations.

8. REFERENCES

[1]https://www.armyrecognition.com/sweden_swedish_missile_systems_and_vehicles_uk/rbs_70_man_portable_air_defense_missile_system_technical_data_sheet_specifications_pictures_video.html, 2018-02-21.

[2] https://www.officer.com/home/article/10248423/tactical-advantages-of-thermal-imaging, 2018-02-21.

[3] Internal document: RBS 70 NG, Saab Dynamics AB, 2012.

[4] Internal document: RBS 70 NG Technical publication suite, Saab Dynamics AB, 2017.

[5] Internal document: RBS 70. Fordonsstativ, kravspecifikation, BOFORS, 1978.

[6] Internal document: Determination of platform stiffness with regard to launch, RBS 70 NGXI, Saab Dynamics AB, 2016.

[7] Steidel. Robert F, An Introduction to Mechanical Vibrations, third ed., John Wiley and Sons, New York, 1989.

[8] J. L. Meriam, L. G. Kraige, Engineering Mechanics: Dynamics, seventh ed., John Wiley and Sons, New York, 2013.

[9] Ali H. Nayfeh, P. Frank Pai, Linear and Nonlinear Structural Mechanics, John Wiley and Sons, Chichester, 2008.

[10] Robert A. Adams, Christopher Essex, Calculus: A Complete Course, eighth ed., Pearson Canada, Toronto, 2013.

[11] Guohai Chen, Jilei Zhou, Dixiong Yang, Benchmark solutions of stationary random vibration for rectangular thin plate based on discrete analytical method, Probabilistic Engineering Mechanics 50 (2017) 17–24.

[12] Eduard Ventsel, Theodor Krauthammer, Thin Plates and Shells, CRC Press Inc, New York, 2001.

[13] https://www.ux1.eiu.edu/~cfadd/1150/06WrkEng/ElPE.html , 2018-05-04.

[14] Internal document: Viktsreduktion VSHORAD NG Stand, Saab Dynamics AB, 2012.

[15] https://studentcommunity.ansys.com/thread/material-damping-and-modal-analysis/, 2018-04-17.

[16] http://www.scielo.br/scielo.php?script=sci_arttext&pid=S1678-58782012000200013, 2018-04-17.

[17] http://www.vibrationresearch.com/university/lesson/what-is-the-psd/, 2018-04-17.

[18] https://www.grc.nasa.gov/www/k-12/airplane/work.html, 2018-05-04.

9. APPENDICES

APPENDIX A

Anslagsdämpare typ C

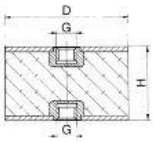

Användningsområde och egenskaper: Cylindriska vibrationsdämpare är enkla och robusta gummielement, 60°Shore. Lämpar sig för användning inom ett stort antal användningsområden, t ex isolering av fläktar, pumpar, luftkonditioneringsanläggningar, apparatskåp, elmotorer, kompressorer etc. Typ C: Med inv gänga/inv gänga.

Tabelldata

Tabellrubrik	Beskrivning
D/H	DiamxHöjd mm B=60°Shore
Gänga	Gänga x längd mm
Tryck K	Tryckbelastning Fjäderkonstant K, kg/mm
Tryck F	Tryckbelastning max F, kg
Skjuv K	Skjuvbelasning Fjäderkonstant K, kg/mm
Skjuv F	Skjuvbelastning max F, kg

Artnr	D/H	Gänga	Tryck K	Tryck F	Skjuv K	Skjuv F	Enh
1042698	C 15/15 B	M4X4	6,5	9,0	1,4	7,0	ST
1042699	C 20/20 B	M6X6	8,5	16,0	1,7	11,5	ST
1042700	C 25/20 B	M6X6	14,5	32,5	3,0	23,5	ST
1042701	C 25/25 B	M6X6	8,0	30,0	2,0	18,0	ST
1042702	C 30/20 B	M8X8	27,5	38,0	4,5	38,0	ST
1042703	C 30/30 B	M8X8	11,5	30,0	2,5	30,0	ST
1042704	C 40/30 B	M8X8	20,0	81,0	5,0	59,0	ST
1042705	C 40/40 B	M8X8	14,5	70,0	3,5	52,0	ST
1042706	C 50/30 B	M10X10	45,0	150,0	8,0	105,0	ST
1042707	C 50/36 B	M10X10	28,0	147,0	7,0	103,0	ST
1042708	C 50/40 B	M10X10	26,0	145,0	5,0	100,0	ST
1042709	C 50/50 B	M10X10	17,5	135,0	4,0	95,0	ST
1042710	C 70/45 B	M10X10	49,0	290,0	9,0	200,0	ST
1042711	C 75/40 B	M12X12	78,0	360,0	12,5	226,0	ST
1042712	C 75/50 B	M12X12	51,0	333,0	9,0	223,0	ST
1042713	C 75/55 B	M12X12	45,0	322,0	8,0	220,0	ST
1042714	C 100/55 B	M16X16	96,0	640,0	16,5	415,0	ST

APPENDIX B

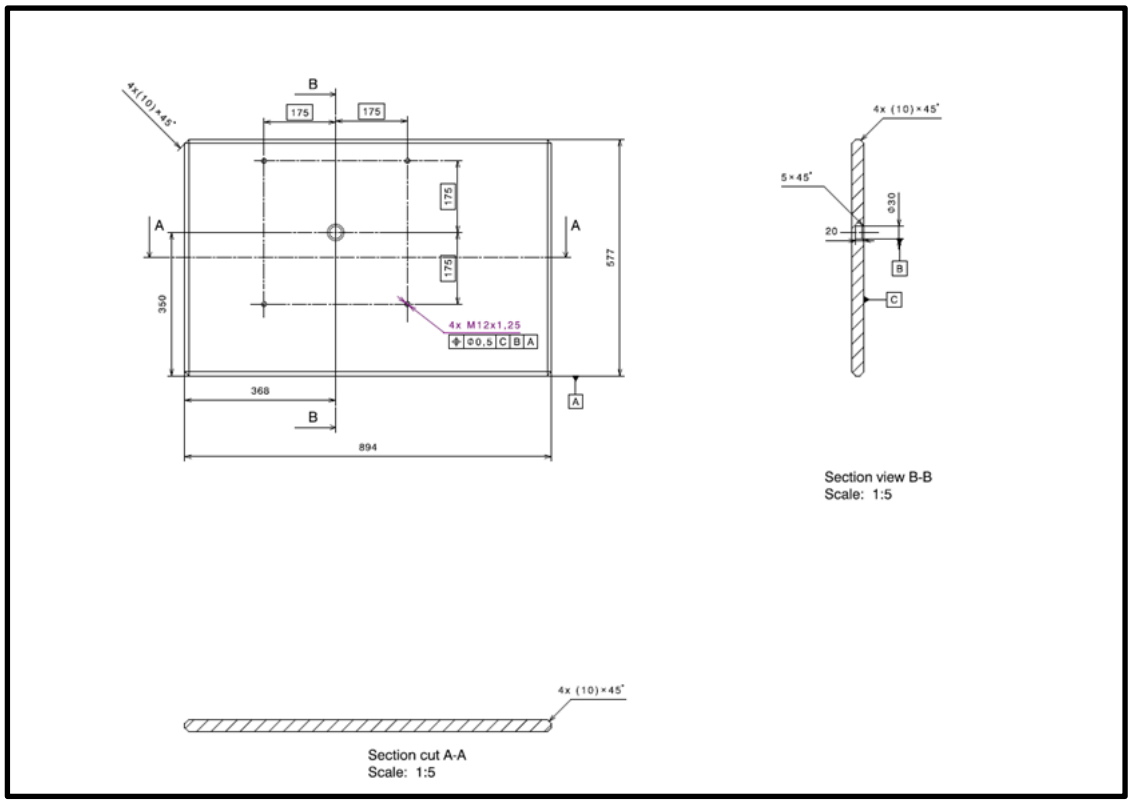
4x (10)×45°
B
175
175
175
175
A
A
350
577
4x M12x1,25
Φ0,5 C B A
368
B
894
A
4x (10)×45°
5×45°
Ø30
20
B
C
Section view B-B
Scale: 1:5
4x (10)×45°
Section cut A-A
Scale: 1:5

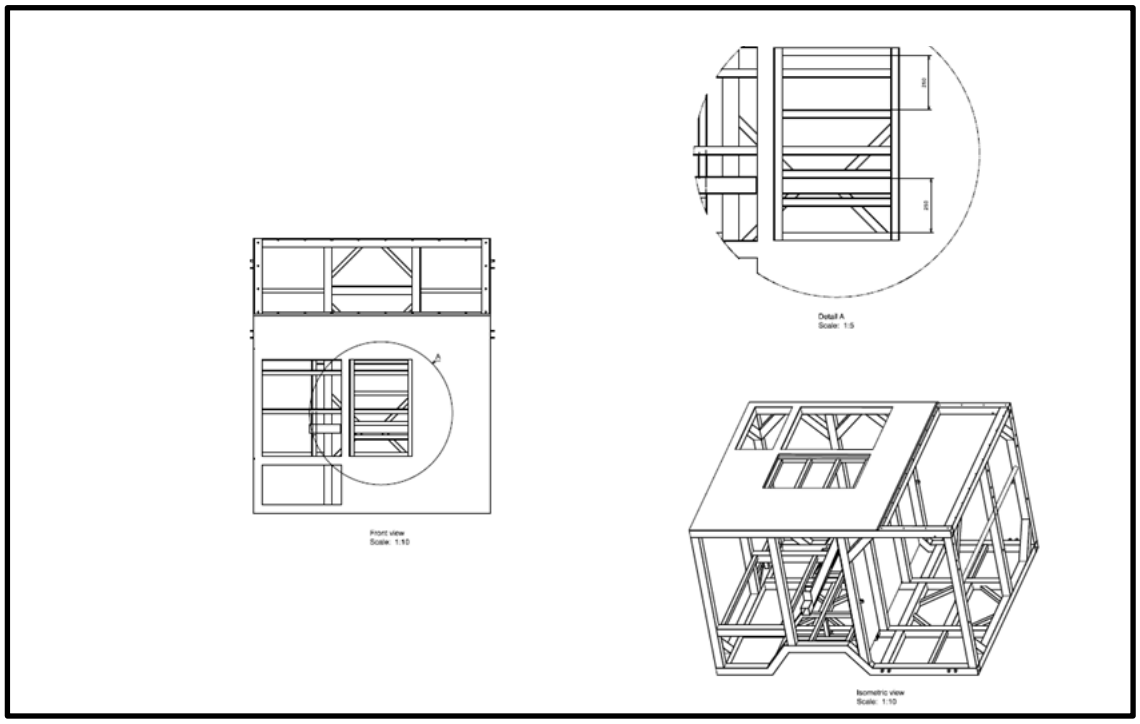
Front view
Scale: 1:10
Detail A
Scale: 1:5
Isometric view
Scale: 1:10